AD-A092 128 MASSACHUSETTS INST OF TECH LEXINGTON LINCOLN LAB F/G 9/2
A NEW ALGORITHM FOR TWO-DIMENSIONAL MAXIMUM ENTROPY POWER SPECT--ETC(U)
AUG 80 J S LIM, N A MALIK F19628-80-C-0002
UNCLASSIFIED TN-1980-37 ESD-TR-80-92 NL

1 OF 1
AD A092 128

END
DATE FILMED
4 81
DTIC

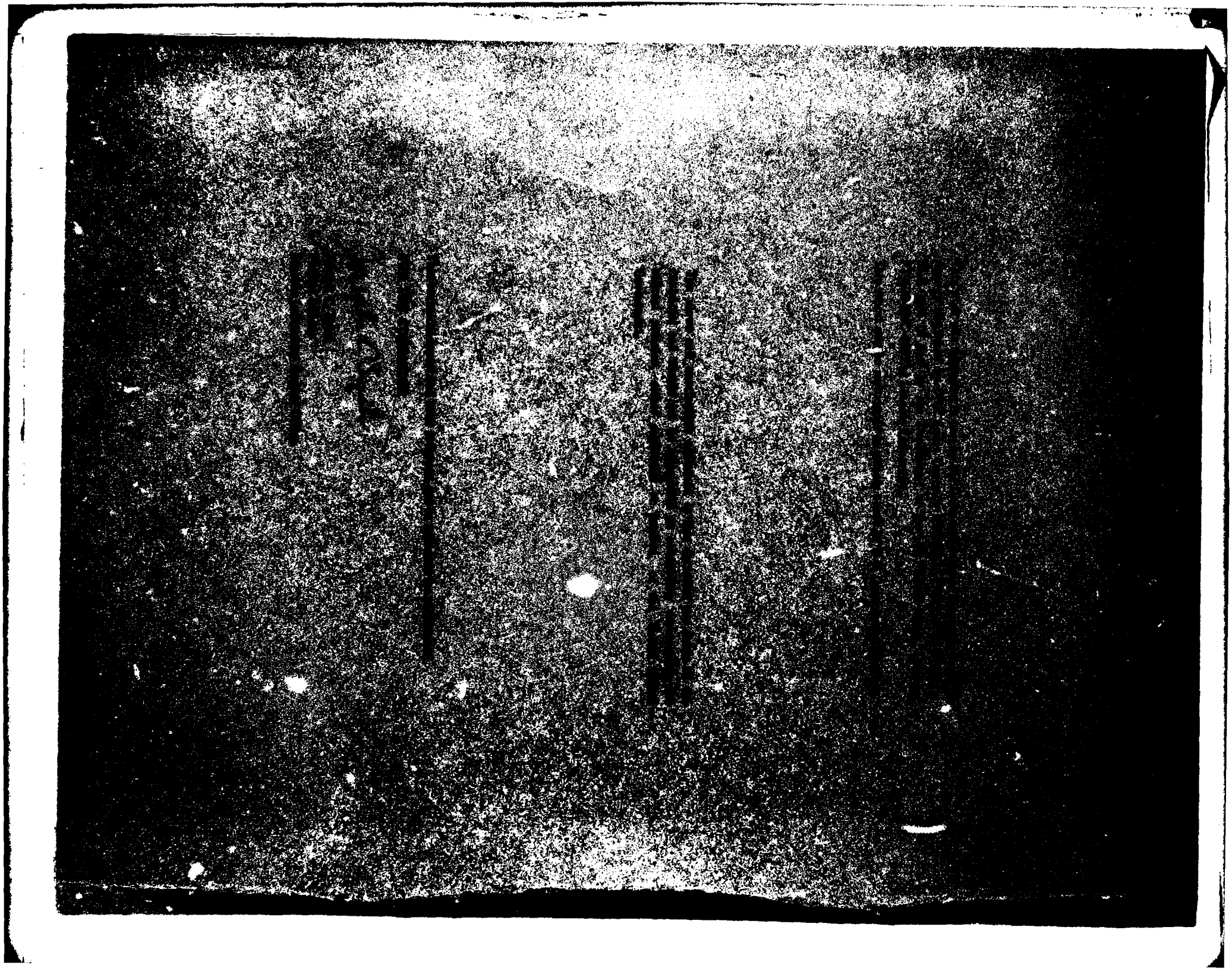

MASSACHUSETTS INSTITUTE OF TECHNOLOGY
LINCOLN LABORATORY

A NEW ALGORITHM FOR TWO-DIMENSIONAL MAXIMUM ENTROPY POWER SPECTRUM ESTIMATION

*J. S. LIM**
*N. A. MALIK**
Group 27

TECHNICAL NOTE 1980-37

7 AUGUST 1980

*The authors are with the M.I.T. Research Laboratory of Electronics and M.I.T. Lincoln Laboratory.

LEXINGTON MASSACHUSETTS

ABSTRACT

A new iterative algorithm for the maximum entropy power spectrum estimation is presented in this report. The algorithm which is applicable to two-dimensional signals as well as one-dimensional signals, utilizes the computational efficiency of the Fast Fourier Transform (FFT) algorithm and has been empirically observed to solve the maximum entropy power spectrum estimation problem. Examples are shown to illustrate the performance of the new algorithm.

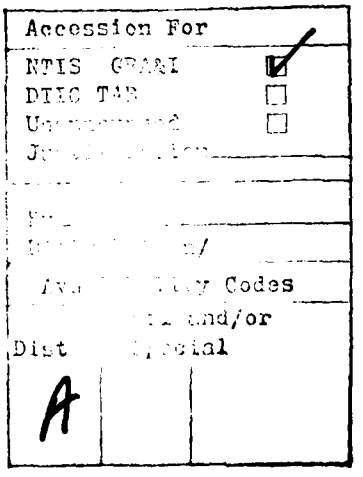

CONTENTS

I. INTRODUCTION

The problem of power spectrum estimation (PSE) arises in various fields such as speech processing [1], seismic signal processing [2], image restoration [3], radar [4], sonar [5], radio astronomy, etc., and its applications range from identifying signal source parameters and transmission channel characteristics to removing noise from images [3]. Consequently, this problem has received considerable attention in the literature and a variety of techniques for power spectrum estimation have been developed.

One technique which has been studied extensively due to its high resolution characteristics is the Maximum Entropy (ME) method. For one-dimensional (1-D) signals, this method is equivalent [7] to auto-regressive signal modelling, and thus it leads to a linear problem formulation that is theoretically tractable and computationally attractive [7]. Unlike most other PSE techniques such as the conventional methods [8,9] and the Maximum Likelihood Method [10], however, the ME method does not extend from 1-D signals to two-dimensional (2-D) signals in a straight-forward manner and the ME method for 2-D signal PSE remains a highly non-linear problem.

To solve the non-linear ME PSE problem for 2-D signals,

various attempts [2,11,12,13] have been made in the literature. In all cases, however, the algorithms are computationally unattractive, and there is no guarantee of a solution or only an approximate solution can be obtained. For example, Burg [11] has proposed an iterative solution which requires the inversion of a matrix in each iteration where the dimension of the matrix is in the order of the number of the given auto-correlation points. No experimental results using this technique have yet been reported. As another example, Wernecke and D'Addario [12] have proposed a scheme in which an attempt is made to numerically maximize the entropy. The maximization is done by continuously adjusting the power spectrum (PS) estimate and evaluating the expressions for the entropy and its gradient. The procedure is computationally expensive and is not guaranteed to have a solution. As a third example, Woods [2] expresses the ME PS estimate as a power series in the frequency domain and attempts to approximate the ME PS estimate by truncating the power series expansion. Even though such an approach has some computational advantages relative to others, the method is restricted to the class of signals for which the power series expansion is possible. Furthermore, examples have been found in which the algorithm does not converge to the desired ME PS estimate.

In this paper, we develop a new iterative algorithm which is computationally simple due to its utilization of the Fast Fourier Transform (FFT) algorithm and which leads to the true ME power spectrum estimate for 2-D signals as well as 1-D signals. In Section II, we review briefly previous results on the ME PSE for 2-D signals. In Section III, we develop a new algorithm for the ME PSE. In Section IV, we illustrate and discuss the performance of this algorithm by way of various examples.

II. PREVIOUS RESULTS ON ME POWER SPECTRUM ESTIMATION FOR 2-D SIGNALS

In this section, we review briefly important previous results relevant to this paper on the ME PSE for 2-D signals. In reviewing these results, we use the following notations:

$x(n_1,n_2)$: a 2-D random signal whose power spectrum we wish to estimate.

$R_x(n_1,n_2)$: auto-correlation function of $x(n_1,n_2)$

$\hat{R}_x(n_1,n_2)$: an estimate of $R_x(n_1,n_2)$

$P_x(\omega_1,\omega_2)$: power spectrum of $x(n_1,n_2)$

$\hat{P}_x(\omega_1,\omega_2)$: an estimate of $P_x(\omega_1,\omega_2)$

$\lambda(n_1,n_2)$: auto-correlation function whose power spectrum is $1/P_x(\omega_1, \omega_2)$

A : a set of points (n_1,n_2) for which $R_x(n_1,n_2)$ is known

F : discrete time Fourier transform

F^{-1} : inverse discrete time Fourier transform

With the above notations, the ME PSE problem can be stated as follows:

Given $R_x(n_1,n_2)$ for $(n_1,n_2)\in A$,

determine $\hat{P}_x(\omega_1,\omega_2)$ such that the entropy H given by

$$H = \int_{\omega_1=-\pi}^{\pi} \int_{\omega_2=-\pi}^{\pi} \log \hat{P}_x(\omega_1,\omega_2)\, d\omega_1\, d\omega_2 \qquad (1)$$

is maximized and

$$R_x(n_1,n_2) = F^{-1}[\hat{P}_x(\omega_1,\omega_2)] \text{ for } (n_1,n_2)\in A \qquad (2)$$

By rewriting $\hat{P}_x(\omega_1,\omega_2)$ *in terms of* $R_x(n_1,n_2)$ for $(n_1,n_2)\in A$ and $\hat{R}_x(n_1,n_2)$ for $(n_1,n_2)\notin A$ and then setting $\frac{dH}{d\hat{R}_x(n_1,n_2)} = 0$ for $(n_1,n_2)\notin A$, it can be shown that the above problem is equivalent to the following:

Given $R_x(n_1,n_2)$ for $(n_1,n_2)\in A$, determine $\hat{P}_x(\omega_1,\omega_2)$ such that $\hat{P}_x(\omega_1,\omega_2)$ is in the form of

$$\hat{P}_x(\omega_1,\omega_2) = \frac{1}{\sum\limits_{(n_1,n_2)\in A}\sum \lambda(n_1,n_2)\cdot e^{-j\omega_1 n_1}\cdot e^{-j\omega_2 n_2}} \tag{3}$$

$$\text{and } R_x(n_1,n_2) = F^{-1}[\hat{P}_x(\omega_1,\omega_2)] \text{ for } (n_1,n_2)\in A \tag{4}$$

The above problem statement for the ME PSE applies, with appropriate dimensionality changes, to all signals regardless of their dimensionality. The solutions to the problem, however, strongly depend on the signal dimensionality. For 1-D signals, the mean square error minimization of the prediction filter based on auto-regressive signal modelling requires solving a set of linear equations for the filter coefficients and the power spectrum obtained from the estimated filter coefficients is identical to the ME PS estimate. For 2-D signals, this is no longer the case. Specifically, even though minimizing the mean square error of the auto-regressive filter still requires solving a set of linear equations, the power spectrum obtained from the estimated filter coefficients is not the ME PS estimate. The reason for this can be seen by examining the form of the normal equations for the filter coefficients in the auto-regressive signal modelling. The derivation of the general form of the normal equations for 2-D signals is analogous to that for 1-D signals and is given by

$$\sum_{(i,j)\in B} \sum a_{ij} R_x(r-i, s-j) = R_x(r,s) \text{ for } (r,s)\in B \qquad (5)$$

where a_{ij} represents the auto-regressive filter coefficients to be estimated, the set B consists of all points where the filter mask has non-zero values, and the power spectrum obtained from a_{ij} is given by

$$\hat{P}_x(\omega_1,\omega_2) = \frac{1}{\left| \sum_{(k,\ell)\in B} \sum a_{k\ell} \cdot e^{-j\omega_1 k} \cdot e^{-j\omega_2 \ell} \right|^2} \qquad (6)$$

From equation (5), for any non-trivial choice of B, that is if B does not consist of a set of collinear points, the size of independent values of $R_x(n_1,n_2)$ required to solve the above set of equations is greater than the size of the filter mask. For example, consider the filter mask shown in Figure 1(a) in which the solid dots represent the range for which a_{ij} is non-zero. In Figure 1(b) is shown the size of independent values of $R_x(n_1,n_2)$ required to solve for a_{ij} in Figure 1(a) by equation (5). Clearly, the number of correlation points needed is greater than the number of filter coefficients. Since the estimated power spectrum given by equation (6) is completely determined by the filter coefficients alone, it does not possess enough degrees of freedom to satisfy equation (4) which is required for the ME PS estimate. Due to this difficulty, a closed form solution for the 2-D ME PSE problem has not yet

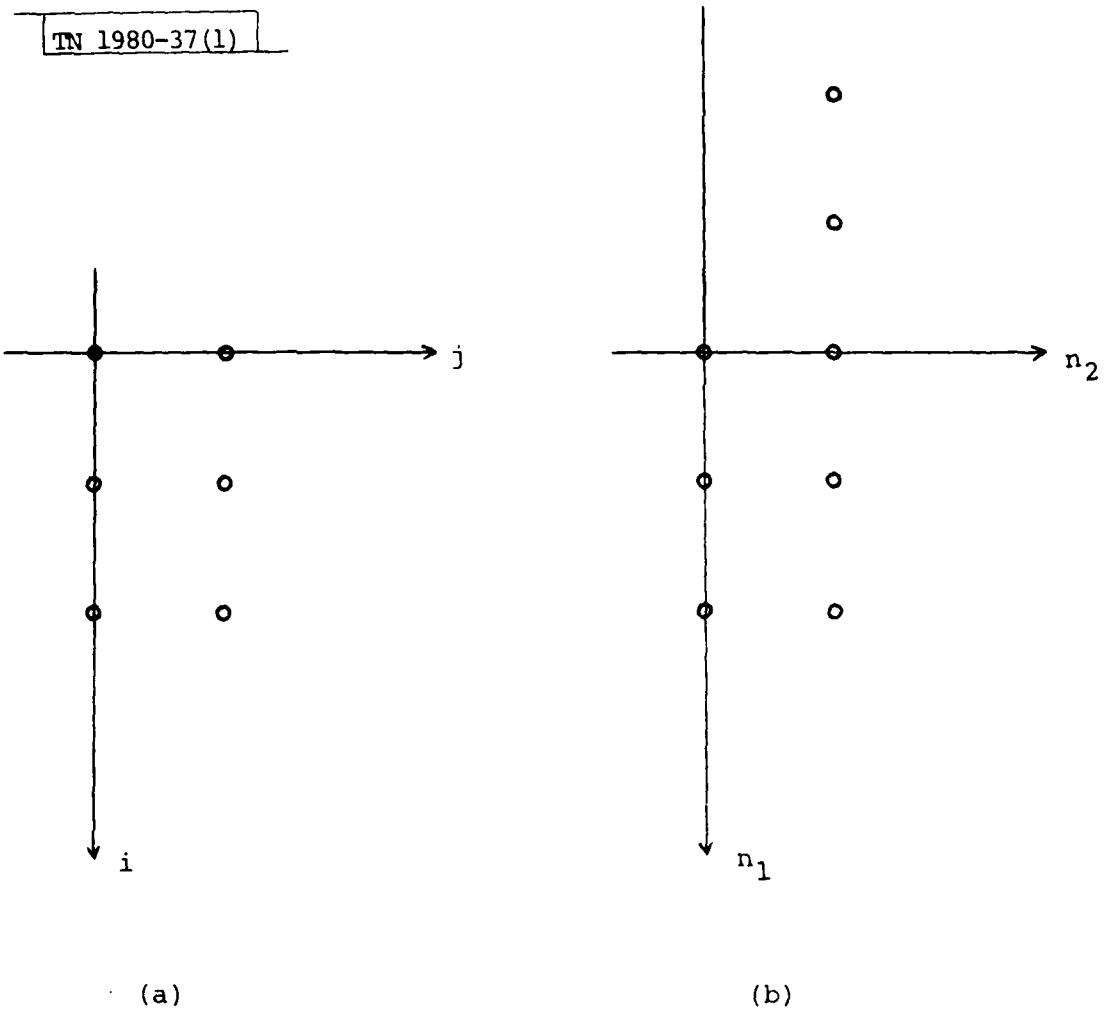

Fig. 1. (a) First quadrant auto-regressive filter mask of size 3x2. (b) Independent auto-correlation points required to solve the normal equations for the mask of (a).

been found.

In the absence of a closed form solution, it is important to know the conditions for the existence and uniqueness of the solution. In this regard, Woods [2] has obtained the theoretical result that if the given $R_x(n_1,n_2)$ for $(n_1,n_2) \epsilon A$ is a part of some positive definite correlation function (meaning that its Fourier transform is positive for all (ω_1,ω_2)), a solution to the ME PSE problem exists and is unique. In general, it is difficult [14] to determine if the given segment of the correlation function is a part of some positive definite correlation function, even though this is generally the case in most practical problems. In this report, we assume that the given segment of the correlation function indeed forms a part of some positive definite correlation function so that the solution to the ME PSE problem exists and is unique.

III. A NEW ITERATIVE ALGORITHM

In this section, we develop a new iterative algorithm for the ME PS estimates which is applicable to both 1-D and 2-D signals. This algorithm is computationally simple since it utilizes the computational efficiency of the FFT algorithm.

Suppose we are given $R_x(n_1,n_2)$ for $(n_1,n_2) \in A$ such that $R_x(n_1,n_2)$ is a segment of some positive definite correlation function. To find the unique ME PS estimate $\hat{P}_x(\omega_1,\omega_2)$, we express a power spectrum $P_y(\omega_1,\omega_2)$ as follows:

$$P_y(\omega_1,\omega_2) = F[R_y(n_1,n_2)]$$

$$= \sum_{n_1=-\infty}^{\infty} \sum_{n_2=-\infty}^{\infty} R_y(n_1,n_2) \cdot e^{-j\omega_1 n_1} \cdot e^{-j\omega_2 n_2} \qquad (7)$$

and $$\frac{1}{P_y(\omega_1,\omega_2)} = F[\lambda(n_1,n_2)]$$

$$= \sum_{n_1=-\infty}^{\infty} \sum_{n_2=-\infty}^{\infty} \lambda(n_1,n_2) \cdot e^{-j\omega_1 n_1} \cdot e^{-j\omega_2 n_2} \qquad (8)$$

From equations (7) and (8), it is clear that $R_y(n_1,n_2)$ can be obtained from $\lambda(n_1,n_2)$ and vice versa through Fourier transform operations. Now, from equations (3) and (4) $P_y(\omega_1,\omega_2)$ is the unique ME PS estimate if and only if $\lambda(n_1,n_2) = 0$ for $(n_1,n_2) \notin A$ and $R_y(n_1,n_2) = R_x(n_1,n_2)$ for $(n_1,n_2) \in A$. Thus, we see that for $P_y(\omega_1,\omega_2)$ to be the desired ME PS estimate, we have a constraint on $R_y(n_1,n_2)$ and a constraint on $\lambda(n_1,n_2)$. Recognizing this, it is straight-forward to develop a simple iterative algorithm to find the unique ME PS estimate. Specifically, we go back and forth between $R_y(n_1,n_2)$ (the correlation domain) and $\lambda(n_1,n_2)$ (the coefficient domain) and

at each time impose the constraints on $R_y(n_1,n_2)$ and $\lambda(n_1,n_2)$. Thus, starting with some initial estimate for $\lambda(n_1,n_2)$ we obtain an estimate for $R_y(n_1,n_2)$. This estimate is then corrected by the given $R_x(n_1,n_2)$ over the region A and is used to generate a new $\lambda(n_1,n_2)$. The new $\lambda(n_1,n_2)$ is then truncated to the desired limits and this procedure is repeated. The above iterative procedure is illustrated in Figure 2 and forms the basis for a new iterative algorithm for the ME PSE.

The iterative procedure discussed above is very similar in form to other iterative techniques [15,16] that have been successfully used in image processing. Even though the conditions under which the algorithm converges are not yet known, if the algorithm converges the converging solution satisifies both equations (3) and (4) and consequently is the desired ME PS estimate.

The algorithm in Figure 2 can not, in general, be used to obtain the ME PS estimate without some modifications due to the spectral zero crossing problem. Specifically, the algorithm in Figure 2 requires two inversions of the spectral estimates in each iteration, and thus the algorithm can not be continued if the power spectrum estimate has a zero crossing at any stage in the iterative procedure. Unfortunately, zero

102455-N

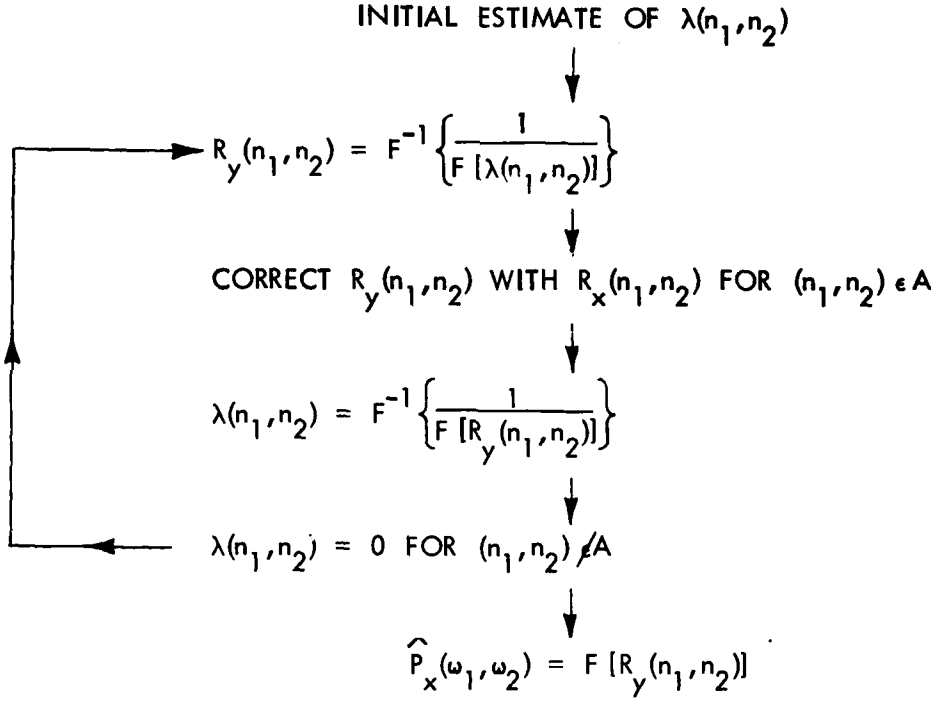

Fig. 2. A new approach to 2-D maximum entropy (ME) power spectrum estimation (PSE).

crossings can occur in two different ways in each iteration. One is the correction of the correlation function and the other is the truncation of the coefficients. To see this, let $\lambda^m(n_1,n_2)$ and $R_y^m(n_1,n_2)$ represent $\lambda(n_1,n_2)$ and $R_y(n_1,n_2)$ after mth iteration and suppose that the following conditions hold;

$$F[\lambda^m(n_1,n_2)] > 0 \text{ for all } (\omega_1,\omega_2), \tag{9}$$

$$F[R_y^m(n_1,n_2)] > 0 \text{ for all } (\omega_1,\omega_2), \tag{10}$$

$$\text{and } \lambda^m(n_1,n_2) = F^{-1}\left[\frac{1}{F[R_y^m(n_1,n_2)]}\right]\cdot w(n_1,n_2) \tag{11}$$

where $w(n_1,n_2)$ represents a rectangular type window such that

$$w(n_1,n_2) = 1 \text{ for } (n_1,n_2)\in A \tag{12}$$

$$0 \text{ otherwise}$$

Similarly, let $\lambda^{m+1}(n_1,n_2)$ and $R_y^{m+1}(n_1,n_2)$ represent $\lambda(n_1,n_2)$ and $R_y(n_1,n_2)$ after m+1th iteration. In the iterative algorithm of Figure 2, $\lambda^{m+1}(n_1,n_2)$ and $R_y^{m+1}(n_1,n_2)$ are obtained from $\lambda^m(n_1,n_2)$ by

$$R'(n_1,n_2) = F^{-1}\left[\frac{1}{F[\lambda^m(n_1,n_2)]}\right], \tag{13}$$

$$R^{m+1}(n_1,n_2) = R_x(n_1,n_2) \text{ for } (n_1,n_2)\in A$$

$$R'(n_1,n_2) \text{ otherwise}$$

$$= R'(n_1,n_2)+(R_x(n_1,n_2)-R'(n_1,n_2))\cdot w(n_1,n_2), \tag{14}$$

$$\lambda'(n_1,n_2) = F^{-1}\left[\frac{1}{F[R_y^{m+1}(n_1,n_2)]}\right], \tag{15}$$

and $\lambda^{m+1}(n_1,n_2) = \lambda'(n_1,n_2)$ for $(n_1,n_2)\epsilon A$

$$0 \quad \text{otherwise}$$

$$= \lambda'(n_1,n_2)\cdot w(n_1,n_2) \tag{16}$$

From equations (13)-(16), it is clear that $R'(n_1,n_2)$ is positive definite since $\lambda^m(n_1,n_2)$ is assumed to be positive definite but $R_y^{m+1}(n_1,n_2)$ may not be positive definite due to the rectangular windowing $w(n_1,n_2)$ in equation (14). Furthermore, even if $R_y^{m+1}(n_1,n_2)$ were positive definite so that $\lambda'(n_1,n_2)$ is positive definite, $\lambda^{m+1}(n_1,n_2)$ may not be positive definite due to $w(n_1,n_2)$ in equation (16).

To ensure the resulting $R^{m+1}(n_1,n_2)$ and $\lambda^{m+1}(n_1,n_2)$ are positive definite so that the iterations can be continued, we make a modification to equation (14). Specifically, instead of forming $R_y^{m+1}(n_1,n_2)$ by replacing $R'(n_1,n_2)$ with all its known values, namely $R_x(n_1,n_2)$ for $(n_1,n_2)\epsilon A$ in equation (14), suppose we form $R_y^{m+1}(n_1,n_2)$ by linearly interpolating between the values of $R'(n_1,n_2)$ and the known values of $R_x(n_1,n_2)$ for $(n_1,n_2)\epsilon A$. Then, in the modified iterative algorithm, $\lambda^{m+1}(n_1,n_2)$ and $R_y^{m+1}(n_1,n_2)$ are obtained from $\lambda^m(n_1,n_2)$ by

$$R'(n_1,n_2) = F^{-1}\left[\frac{1}{F[\lambda^m(n_1,n_2)]}\right] \tag{17}$$

$$R_y^{m+1}(n_1,n_2) = \alpha \cdot R'(n_1,n_2) + (1-\alpha) \cdot R_x(n_1,n_2) \text{ for } (n_1,n_2) \in A$$

$$R'(n_1,n_2) \quad \text{otherwise}$$

$$= R'(n_1,n_2) + (1-\alpha) \cdot (R_x(n_1,n_2) - R'(n_1,n_2))$$

$$\cdot w(n_1,n_2) \tag{18}$$

$$\lambda'(n_1,n_2) = F^{-1}\left[\frac{1}{F[R_y^{m+1}(n_1,n_2)]}\right] \tag{19}$$

and $$\lambda^{m+1}(n_1,n_2) = \lambda'(n_1,n_2) \cdot w(n_1,n_2) \tag{20}$$

Comparing equations (14) and (18), equation (18) reduces to equation (14) when $\alpha = 0$. With any other choice of α, equation (18) represents a non-ideal correction of $R'(n_1,n_2)$ with the known values $R_x(n_1,n_2)$ for $(n_1,n_2) \in A$, with a larger deviation of α from zero corresponding to a more non-ideal correction. However, with proper choice of α, the resulting $R_y^{m+1}(n_1,n_2)$ and $\lambda^{m+1}(n_1,n_2)$ can be guaranteed to be positive definite. This can be seen by noting that $\lambda^m(n_1,n_2)$ and therefore $R'(n_1,n_2)$ are assumed to be positive definite and by considering α sufficiently close to 1 so that $R_y^{m+1}(n_1,n_2)$ and $\lambda^{m+1}(n_1,n_2)$ can be made arbitrarily close to $R'(n_1,n_2)$ and $\lambda^m(n_1,n_2)$. Therefore by properly choosing α in the range $0 \leq \alpha < 1$, the spectral zero crossing problem can be avoided and the iterations can be continued.

From equations (13)-(16), it is clear that if $\lambda^m(n_1,n_2)$ and $R_y^m(n_1,n_2)$ satisfy equations (9)-(11), then $\lambda^{m+1}(n_1,n_2)$ and $R_y^{m+1}(n_1,n_2)$ obtained by the modified iterative algorithm also satisfy equations (9)-(11). With proper choice of α, then, if $\lambda^0(n_1,n_2)$ and $R_y^0(n_1,n_2)$, the initial estimates of $\lambda(n_1,n_2)$ and $R_y(n_1,n_2)$, satisfy equations (9)-(11), the iterations specified by equations (9)-(12) and (17)-(20) form an iterative algorithm. This algorithm is shown in Figure 3.

In implementing the algorithm in Figure 3, there are several important issues that need to be discussed. One of them is the determination of the length of the Discrete Fourier Transform (DFT) and Inverse Discrete Fourier Transform (IDFT) to be used for the Fourier transform and inverse Fourier transform operations. In general, a large DFT length should be used in the implementation to avoid any aliasing problem. Specifically, the ME method of PSE is essentially an attempt to extrapolate the correlation function beyond the limits of the known segment. Since the DFT is used in the implementation instead of the true Fourier transform, the length of the DFT should be chosen such that the extended correlation function corresponding to the ME PS estimate is essentially zero beyond the DFT limits. Choice of the DFT length and its effect on the system performance will be further discussed in Section IV.

102454-N

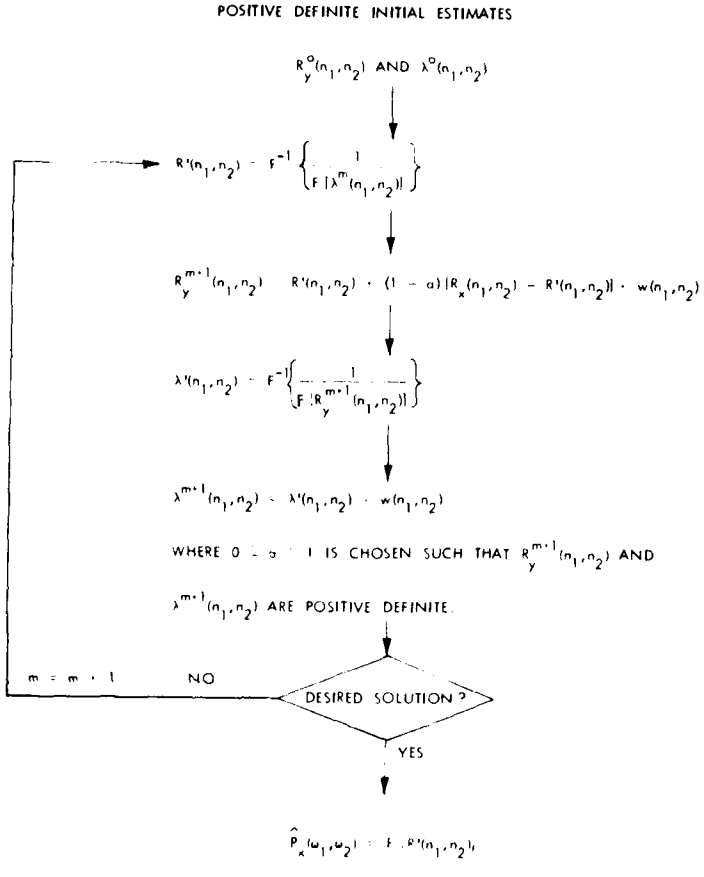

Fig. 3. An iterative algorithm for 2-D ME PSE based on Fig. 2.

Another issue to be considered in the implementation is determination of $\lambda^0(n_1,n_2)$ and $R_y^0(n_1,n_2)$, the initial estimates of $\lambda(n_1,n_2)$ and $R_y(n_1,n_2)$. Even though various different choices are possible, one choice which is particularly simple and satisfies equations (9)-(11) is

$$R_y^0(n_1,n_2) = R_x(0,0)\cdot\delta(n_1,n_2) \tag{21}$$

$$\text{and } \lambda^0(n_1,n_2) = \frac{1}{R_x(0,0)}\cdot\delta(n_1,n_2) \tag{22}$$

where it is assumed that the region A includes the point $(n_1,n_2) = (0,0)$ and that $R_x(0,0) > 0$. Furthermore, the choice of $\lambda^0(n_1,n_2)$ and $R_y^0(n_1,n_2)$ given by equations (21) and (22) is reasonable in that $R_y^m(n_1,n_2) = R_x(n_1,n_2)\cdot w(n_1,n_2)$ for $m = 1$ and $\alpha = 0$ in the iterative algorithm of Figure 3.

A third issue to be discussed in the implementation is how the value of α is specifically determined in each iteration. The choice of α is dictated by two considerations. One is the requirement that the resulting $R_y^{m+1}(n_1,n_2)$ and $\lambda^{m+1}(n_1,n_2)$ are positive definite. The second is our desire to choose α as close to zero as possible so that more correction with the known correlation points is made in each iteration. Thus, the ideal choice of α is the smallest α in the range $0 \leq \alpha < 1$ for which the resulting $R_y^{m+1}(n_1,n_2)$ and $\lambda^{m+1}(n_1,n_2)$ are

positive definite. Finding the optimum value of α, however, may require many iterations in which we begin with $\alpha = 0$ and successively increase α until the resulting $R_y^{m+1}(n_1,n_2)$ and $\lambda^{m+1}(n_1,n_2)$ are positive definite. Since each iteration requires one DFT and one IDFT, obtaining α alone can be a significant computational burden. Further, it has been empirically determined that choosing the smallest α in each iteration can lead to a limit cycle behavior where the algorithm does not converge to the ME PS estimate.

An alternative approach to the choice of α, which avoids the above two problems and is used in this paper, is to begin with $\alpha_0 = 0$ and change α *in the following manner;*

$$\alpha_{m+1} \leftarrow \max\left[\alpha_m, 1-k\cdot\frac{\min\limits_{(\omega_1,\omega_2)}\left[F[R'(n_1,n_2)]\right]}{\left|\min\limits_{(\omega_1,\omega_2)} F[(R_x(n_1,n_2)-R'(n_1,n_2))\cdot w(n_1,n_2)]\right|}\right] \tag{23}$$

$$\text{if} \quad \min_{(\omega_1,\omega_2)}\left[F[(R_x(n_1,n_2)-R'(n_1,n_2))\cdot w(n_1,n_2)]\right] < 0$$

and $\alpha_{m+1} \leftarrow \alpha_m$ otherwise,

where α_i represents the value of α in the ith iteration, $\max[\ ,\ ]$ represents the maximum of the two arguments, $\min\limits_{(\omega_1,\omega_2)}[\ ]$ represents the minimum of the argument expression over (ω_1,ω_2), and "k" is a scalar constant with $0<k\leq 1$. Typically, "k" is

chosen to be 0.01, but can be increased to 1 for low S/N ratio cases. When α is chosen according to equation (23), it is straight-forward to show from equation (14) that the resulting $R_y^{m+1}(n_1,n_2)$ is always positive definite. In addition, it has been empirically observed that the resulting $\lambda^{m+1}(n_1,n_2)$ is almost always positive definite. In those rare cases when $\lambda^{m+1}(n_1,n_2)$ is not positive definite, α is further increased and the iterations continue with the increased α.

Finally, another important issue to be considered in implementing the algorithm in Figure 3 is the decision on when the algorithm converged so that the iteration can be stopped. One reasonable approach is to consider that the algorithm has converged when the following condition is satisfied.

$$\frac{\sum\sum_{(n_1,n_2)\in A} (R'(n_1,n_2)-R_x(n_1,n_2))^2}{\sum\sum_{(n_1,n_2)\in A} R_x^2(n_1,n_2)} \leq \varepsilon \qquad (24)$$

clearly, if $\varepsilon = 0$ and the algorithm has converged, then the converging solution corresponds to the desired ME PS estimate. However, due to a finite DFT length and finite precision arthematic used, it is not possible to reduce the error exactly to zero. A convergence decision is made when the error

ε is very small, typically 10^{-4}.

In Figure 4 is shown a more detailed flow chart of an algorithm which incorporates the important implementation issues discussed above. It is not theoretically known under what conditions the algorithm in Figure 4 converges. As will be discussed in the next section, however, we have empirically observed that the algorithm always converges to the ME PS estimate with a sufficiently large choice of the DFT length and a sufficiently small choice of ε.

IV. EXAMPLES AND DISCUSSIONS

In this section, we illustrate and discuss various examples in which the algorithm in Figure 4 has been applied to obtain the ME PS estimate. In all cases, it was assumed that the correlation function originated from sinusoids buried in white noise so that the correlation function given has the form of

$$R_x(n) = \sigma^2 \cdot \delta(n) + \sum_{i=1}^{M} a_i^2 \cdot \cos(\omega_i n) \quad \text{for 1-D signals} \tag{25}$$

and $$R_x(n_1,n_2) = \sigma^2 \cdot \delta(n_1,n_2) + \sum_{i=1}^{M} a_i^2 \cdot \cos(\omega_{i1} \cdot n_1 + \omega_{i2} \cdot n_2)$$

$$\text{for 2-D signals} \tag{26}$$

where σ^2 represents the white noise power, M represents the

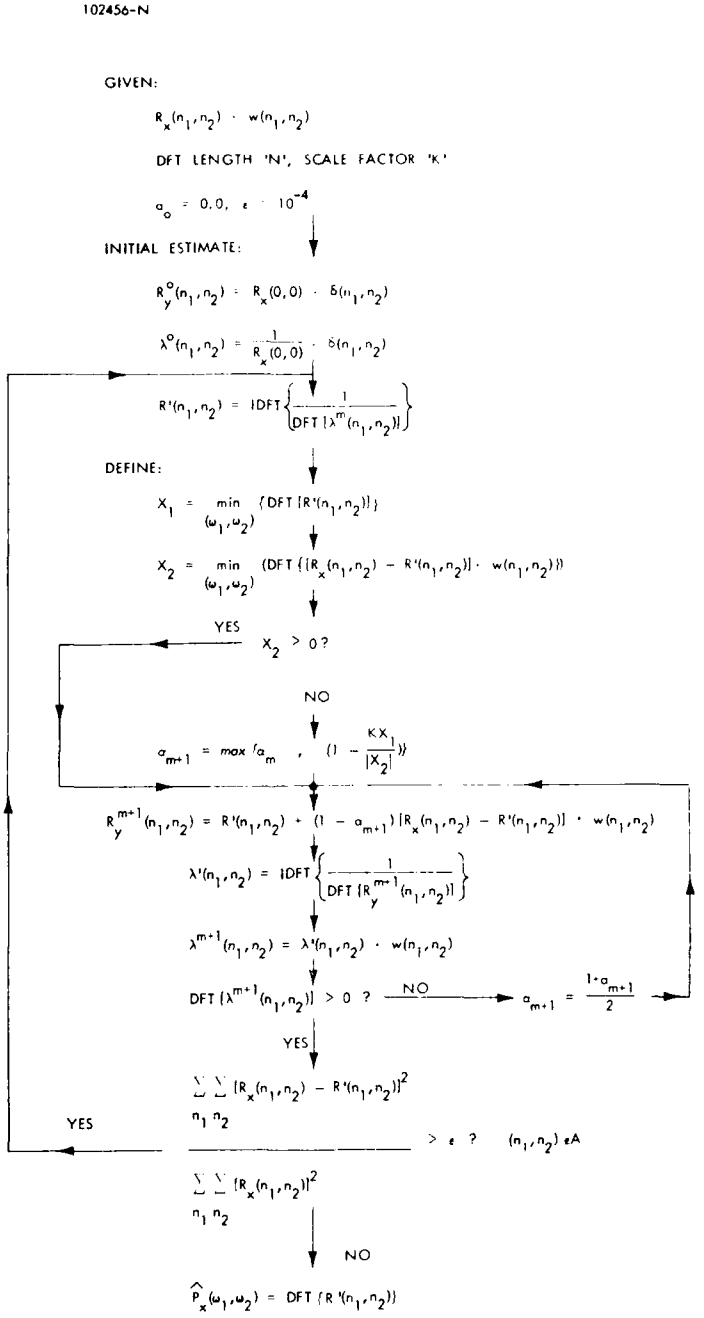

Fig. 4. A detailed flow-chart of the iterative algorithm for 2-D ME PSE implemented in this paper.

number of sinusoids, a_i^2 represents the power of the ith sinusoid, and ω_i for 1-D signals and ω_{i1} and ω_{i2} for 2-D signals represent the frequencies of the ith sinusoid.

We first consider the case of 1-D signals. For 1-D signals, the iterative algorithm in Figure 4 is not very useful in obtaining the ME PS estimate due to the existence of a simple closed form solution. However, the 1-D signal case is ideal in illustrating that the solution obtained from the iterative algorithm in Figure 4 indeed leads to the ME PS estimate. In Figure 5 are shown the results obtained using the parameters in Table 1. In Figure 5(a) are shown the results obtained from the iterative algorithm as a function of the number of iterations. The converging solution with the choice of ε in Table 1 was obtained after 200 iterations. In Figure 5(b) is shown the ME PS estimate obtained from the closed form solution of equation (6). Figure 5(c) shows the PS estimates obtained from the iterative algorithm (solid line) and the closed form solution (dotted line). It is clear from Figure 5(c) that the iterative algorithm leads to the ME PS estimate.

As another 1-D example, Figure 6 is similar to Figure 5 except that the parameters in Table 2 were used to generate the results. In addition to the above two examples, a variety of other examples have been considered. In all cases

TABLE 1

Parameters of a one-dimensional example for Figure 5.

A	M	σ^2	a_i^2	$\omega_1/2\pi$	ε	NDFT	NITR	TIME
9	1	1.0	1.0	0.1 0.3456	10^{-4}	128	200	3 secs.

A : size of the known auto-correlation array, symmetric about the origin

M : number of sinusoids

σ^2 : noise power

a_i^2 : power of ith sinusoid

ω_i : frequency of ith sinusoid

ε : error used for the convergence test

NDFT : size of discrete Fourier transform used

NITR : number of iterations required to reach ε

Time : the CPU time required using IBM-370 at M.I.T. Lincoln Laboratory

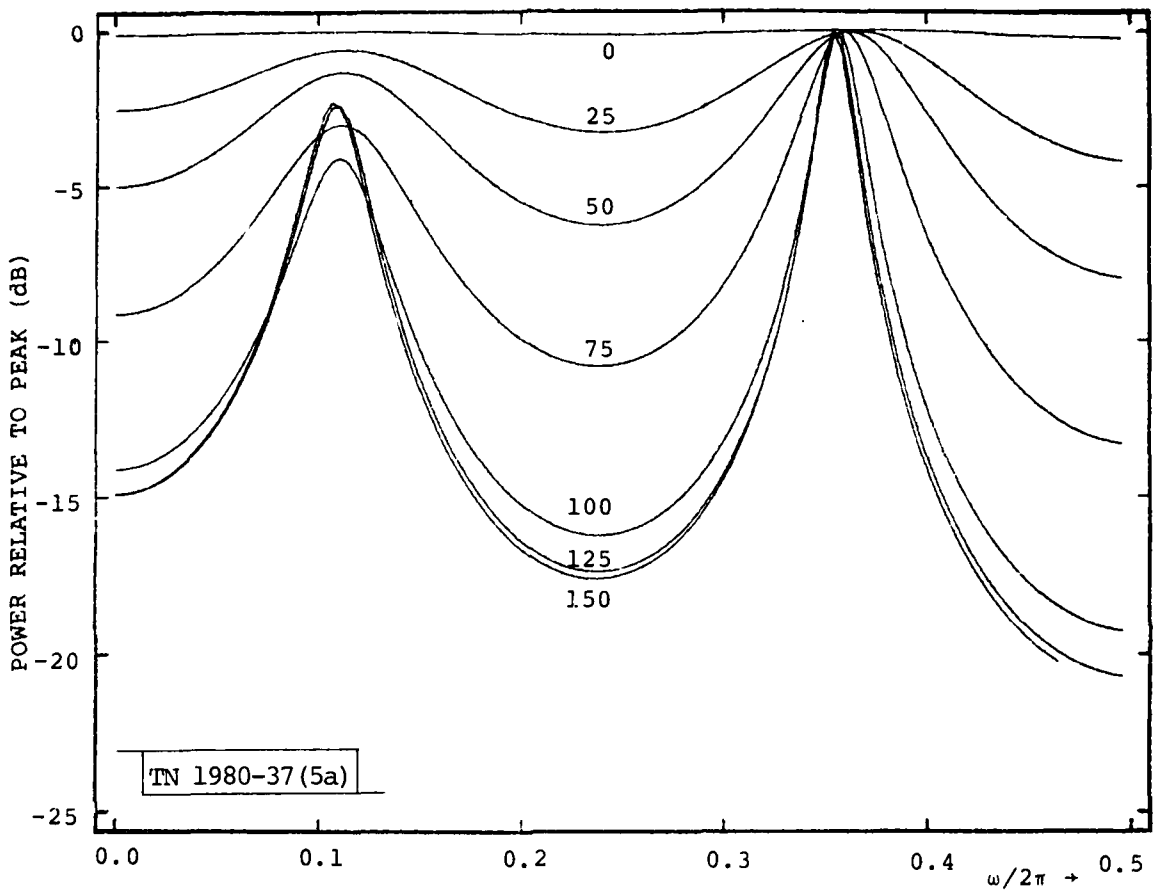

(a) The PS estimate as a function of the number of iterations (NITR). NITR = 0, 25, 50, 75, 100, 125, 150.

Fig. 5. 1-D PSE for the data in Table 1.

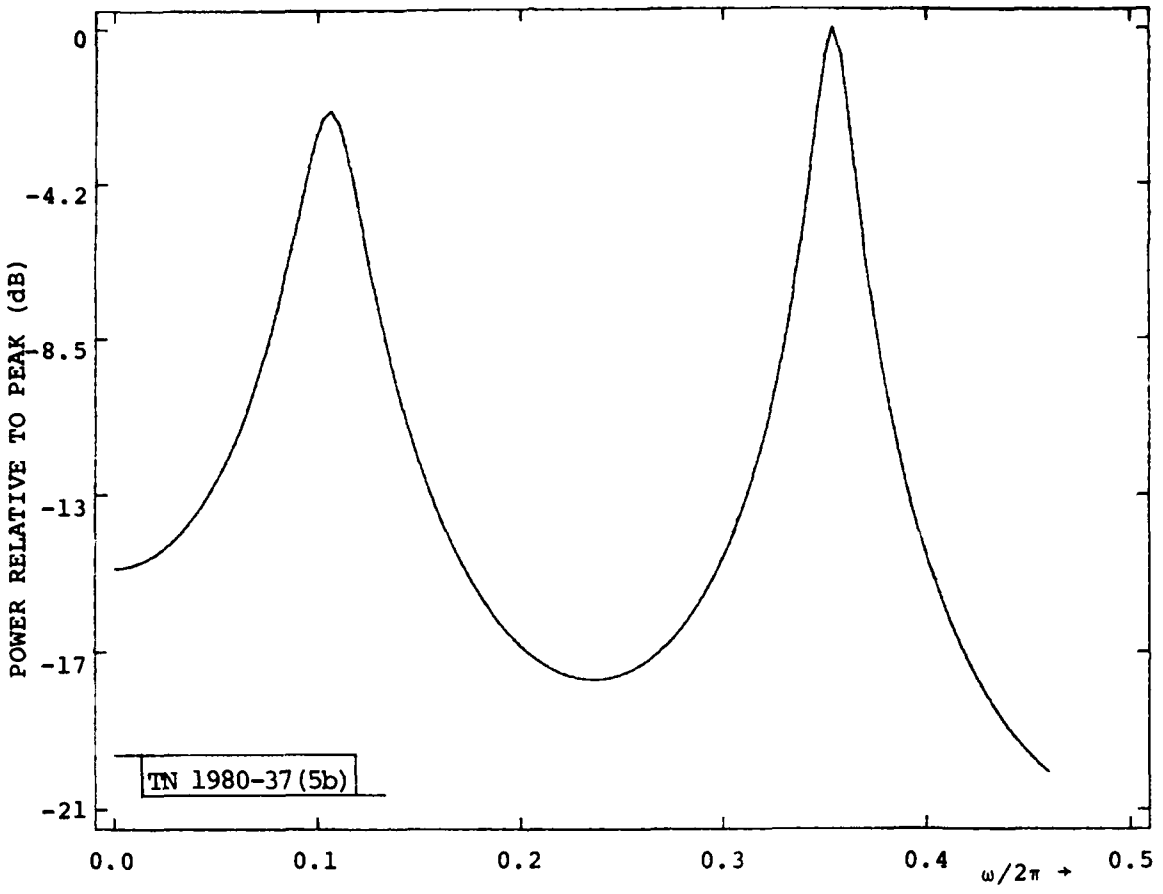

(b) Results of ME PSE by the closed form solution of equations (5) and (6).

Fig. 5. Continued.

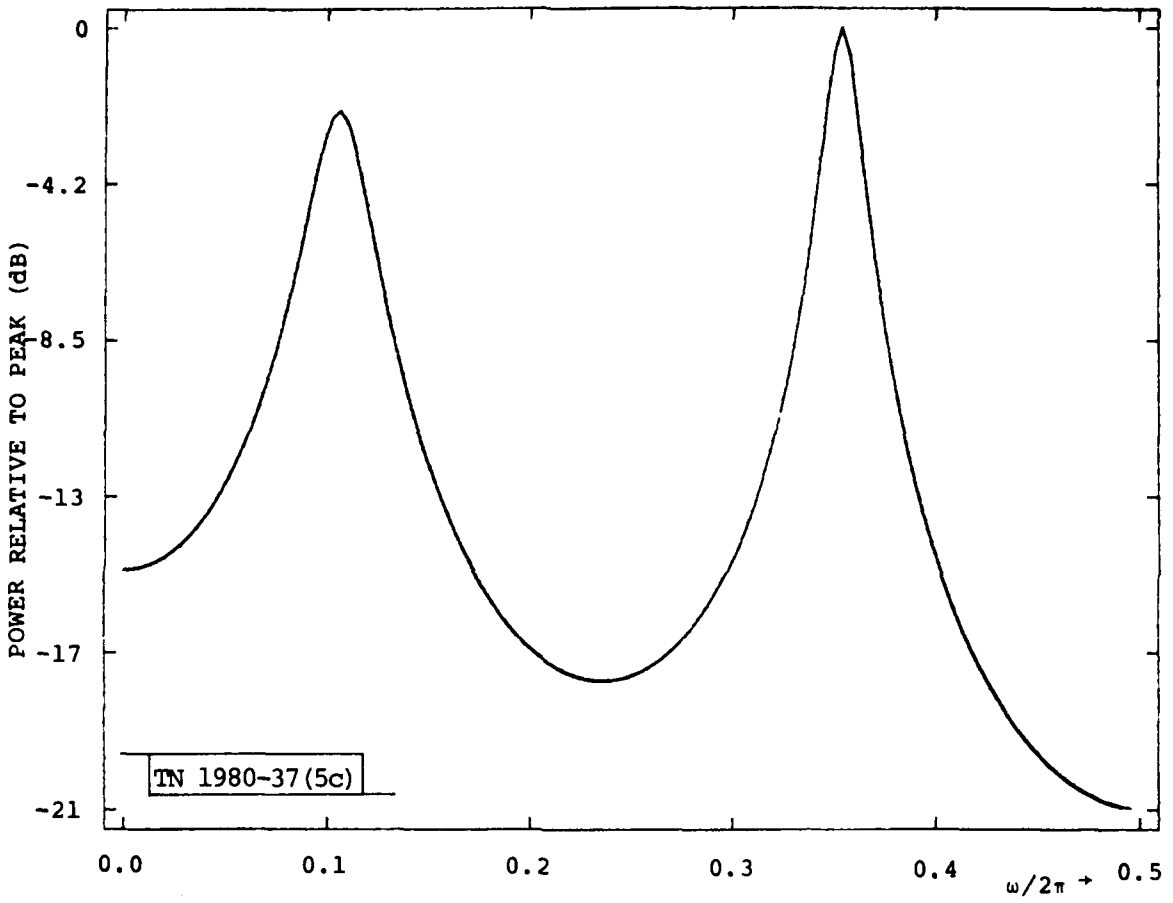

(c) Result of the iterative method (solid line). Result of the closed form solution (dotted line). The two results are indistinguishable.

Fig. 5. Continued.

that we have considered so far, the iterative algorithm in Figure 4 lead to the PS estimates which are visually indistinguishable from the closed form solutions.

TABLE 2

Parameters of a one-dimensional example for Figure 6. Notations used in the table are explained in Table 1.

A	M	σ^2	a_i^2	$\omega_i/2\pi$	ε	NDFT	NITR	Time
5	1	1.0	10	0.1	10^{-4}	64	69	less than 1 sec.

We now consider the case of 2-D signals. For 2-D signals, a closed form solution for ME PSE has not yet been found and consequently the iterative algorithm developed in this paper has practical significance. In Figure 7 are shown the results obtained using the parameters in Table 3. In Figure 7(a) is shown the periodogram [9] obtained by Fourier transforming $R_x(n_1,n_2)\cdot w(n_1,n_2)$. In Figure 7(b) is shown the PS estimate based on auto-regressive signal modelling of equation (6) using a backward L shaped filter mask [16]. This particular mask was chosen due to its high performance [16] relative to other filter mask shapes such as symmetric and first quadrant filters. In

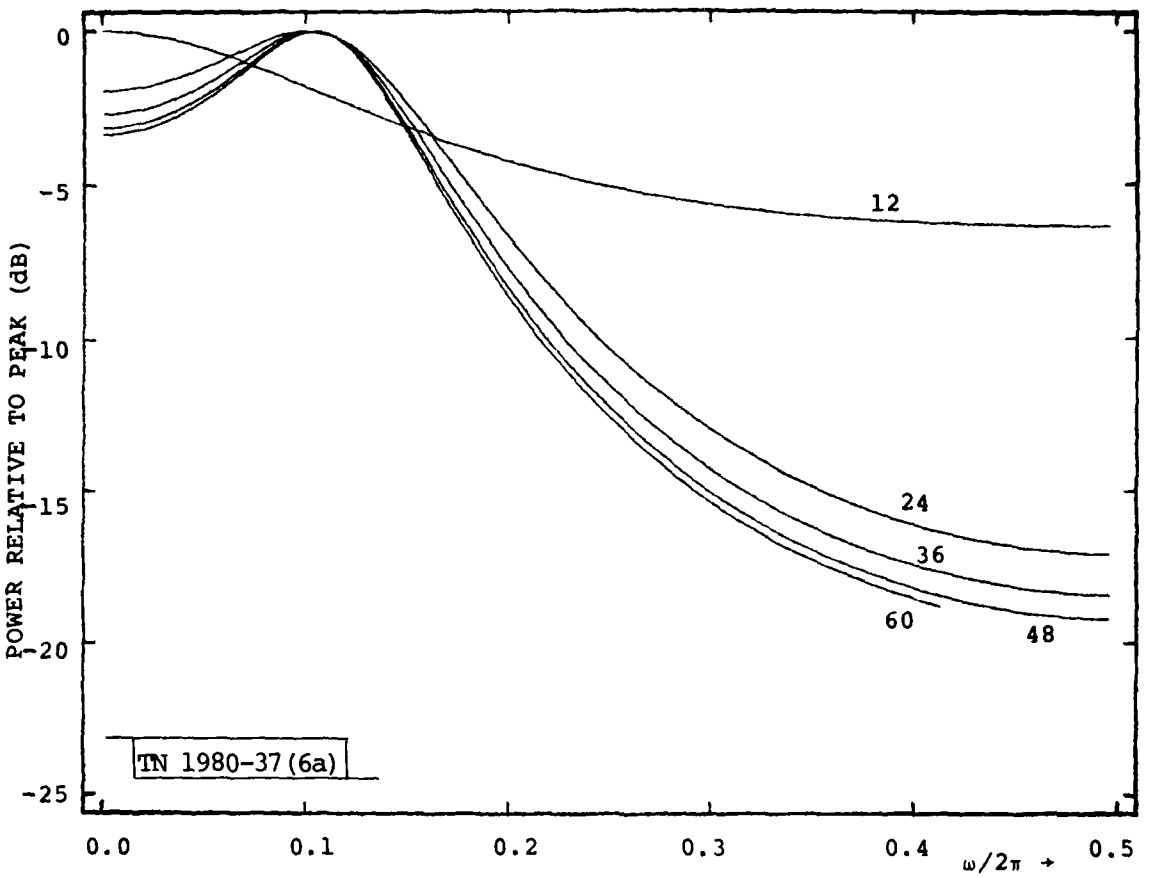

(a) The PS estimate as a function of NITR.
NITR = 12, 24, 36, 48, 60.

Fig. 6. 1-D PSE for the data in Table 2.

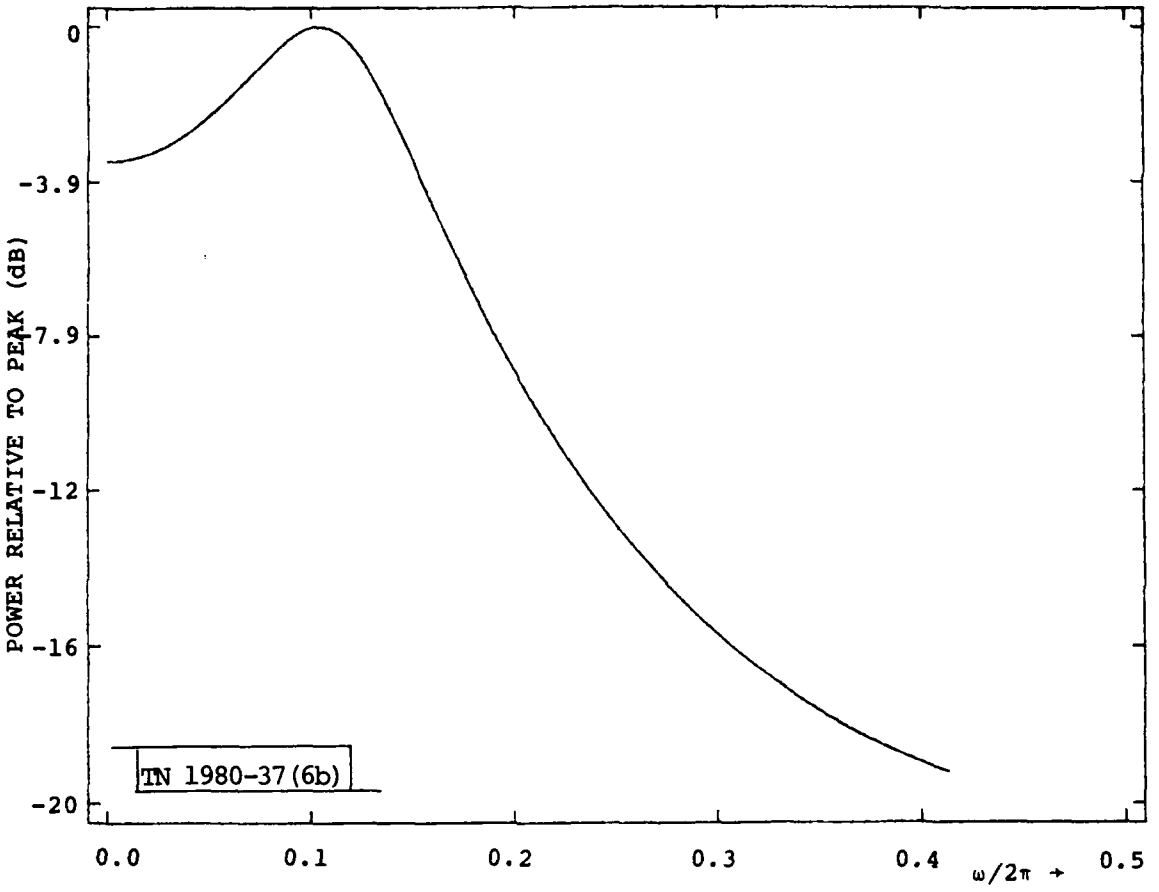

(b) Result of ME PSE by the closed form solution of equations (5) and (6).

Fig. 6. Continued.

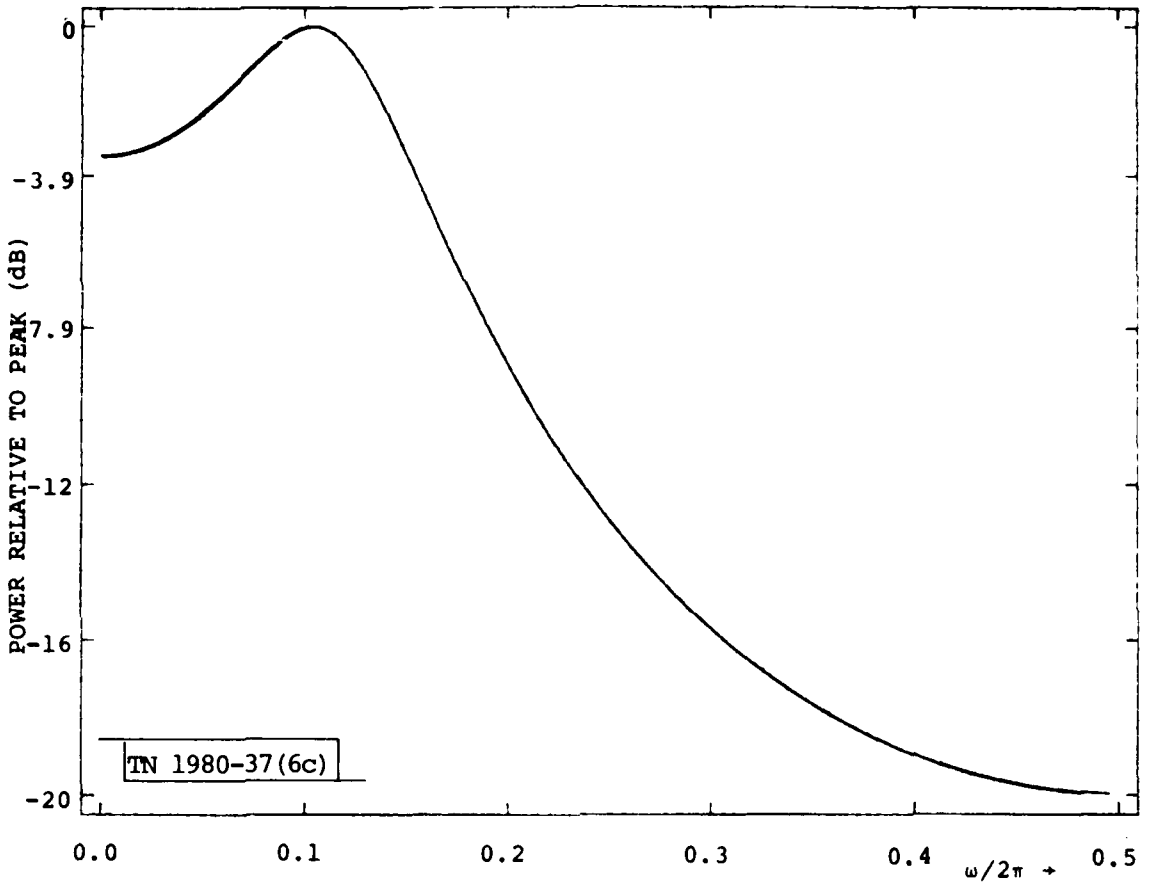

(c) Result of the iterative method (solid line). Result of the closed form solution (dotted line). The two results are indistinguishable.

Fig. 6. Continued.

Figure 7(c) is shown the PS estimate obtained from the iterative algorithm developed in this paper. To ensure that the PS estimate shown in Figure 7(c) corresponds to the ME PS estimate, an additional estimate was obtained using a larger DFT size of 128×128 points and a much smaller ϵ of 10^{-6} and was compared to the result in Figure 7(c). The two estimates were visually indistinguishable. It is clear from Figure 7 that the two sinusoids are resolved only in Figure 7(c), implying that the ME method for PSE has the high resolution characteristics for 2-D signals as well as 1-D signals.

TABLE 3

Parameters of a two-dimensional example for Figure 7. Notations used in the table are explained in Table 1.

A	M	σ^2	a_i^2	$(\omega_{i1}/2\pi, \omega_{i2}/2\pi)$	ϵ	NDFT	NITR	Time
5×5	2	1.0	1.0 1.0	0.10 0.10 0.20 0.3125	10^{-4}	64×64	199	75 secs.

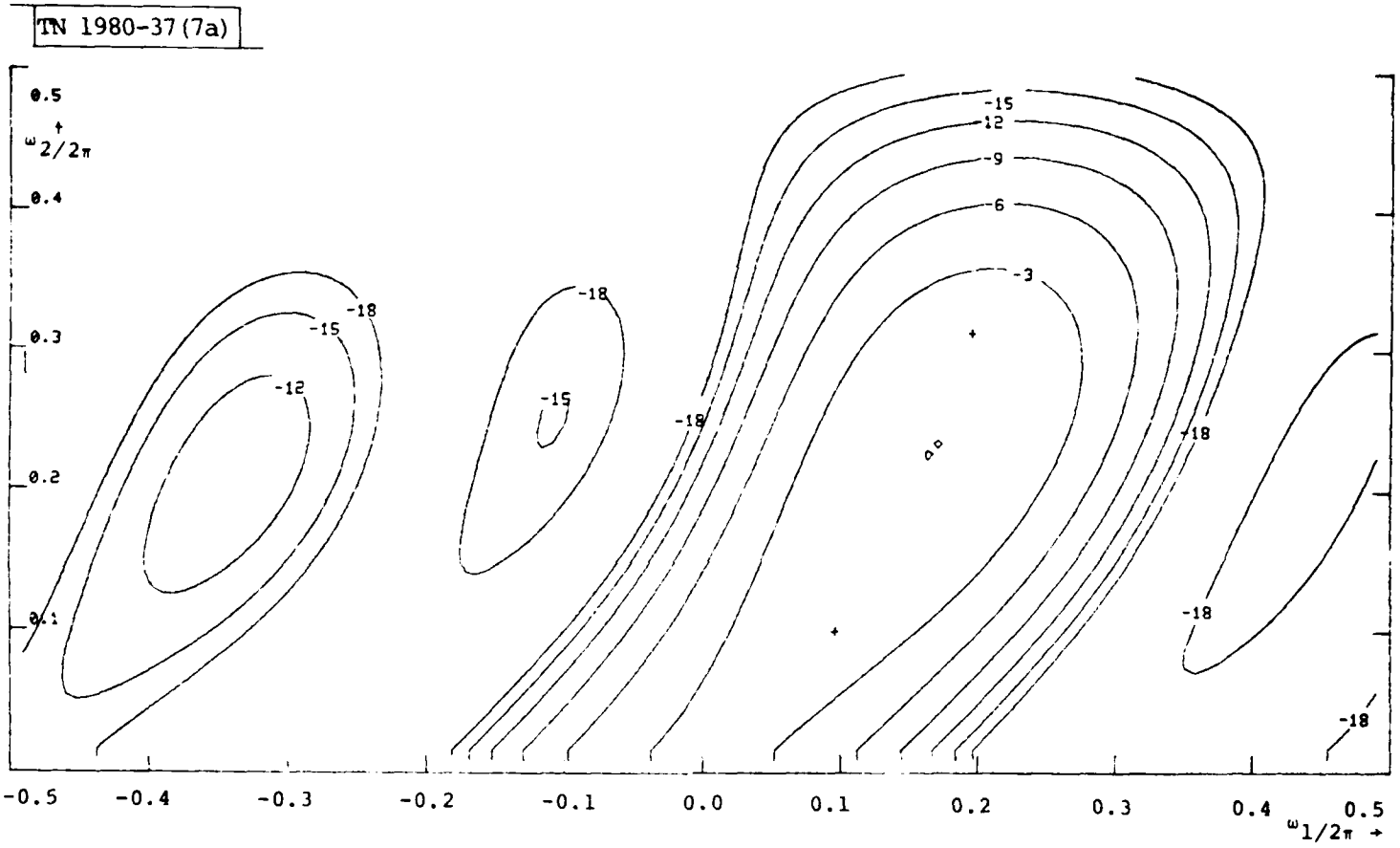

(a) Result of PSE by periodogram.

Fig. 7. 2-D PSE for data in Table 3. "+" in all figures represent the true peak locations of the signal sinusoids and the numbers on the countors represent "dB" relative to the maximum value of the estimated power spectrum.

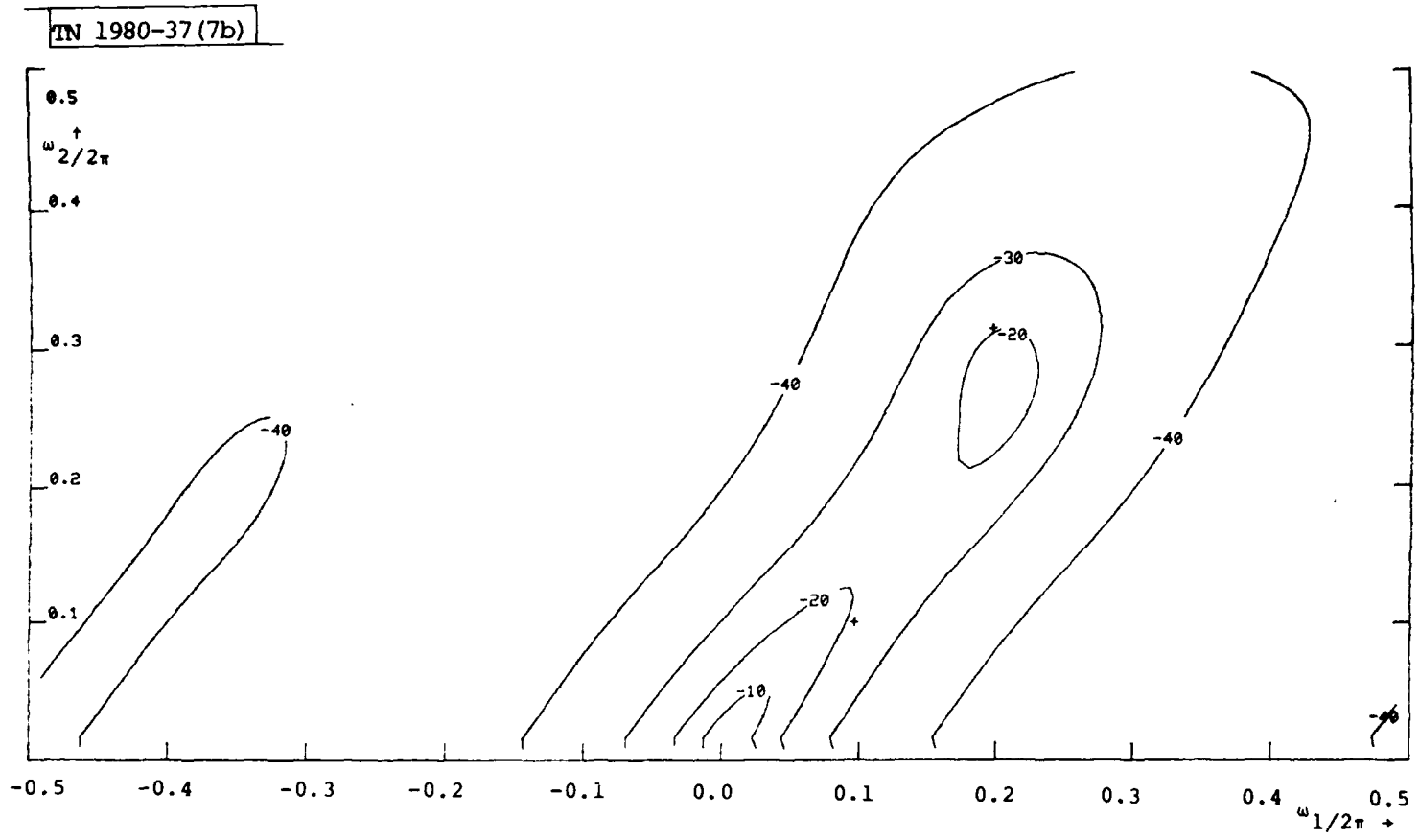

(b) Result of PSE based on the backward L auto-regressive filter.

Fig. 7. Continued.

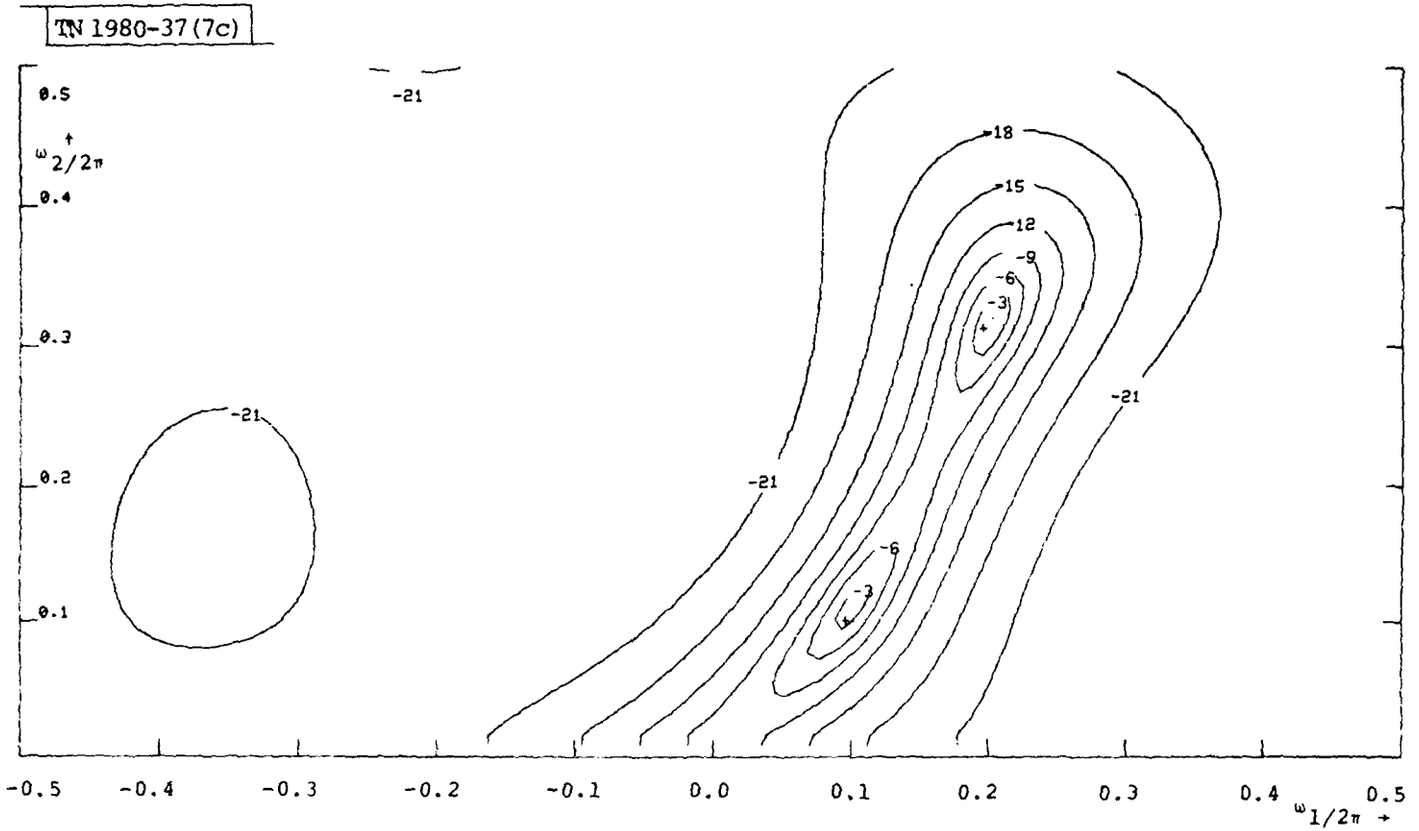

(c) ME PS estimate by the iterative algorithm in Fig. 4.

Fig. 7. Continued.

In using the iterative algorithm developed in this paper, care should be exercised in properly choosing the DFT length. As has been discussed in Section III, a smaller aliasing error requires a longer DFT. However, once the DFT length is chosen so that the aliasing error is sufficiently small relative to ε, a further increase in the DFT length makes little improvement in the spectral estimates, but only increases the computational requirements. To give a rough estimate of the DFT length needed in practice, a number of examples have been considered and the ranges of DFT lengths required for $\varepsilon = 10^{-4}$ have been computed as a function of the S/N ratio and the size of A. The S/N ratio in dB is defined as

$$\text{S/N ratio in dB} \triangleq 10 \cdot \log\left(\frac{\sum_{i=1}^{M} |a_i|^2}{\sigma^2}\right) \tag{27}$$

and the computed results are shown in Table 4.

TABLE 4

Typical ranges of minimum DFT size needed in practice to achieve convergence of the algorithm in Figure 4 with $\varepsilon = 10^{-4}$.

S/N ratio	Size of A			
	1-D Signals		2-D Signals	
	5	9	3×3	5×5
-10 db	8-16	8-32	8×8	8×8 - 16×16
0 db	16-64	32-128	8×8 - 16×16	16×16 - 64×64
+10db	64-512	64-1024	32×32-256×256	64×64-512×512

From Table 4, it is clear that cases in which the S/N ratio is higher or the size of A is larger require longer DFTs. This is due to the fact that the correlation functions given in equations (25) and (26) represent more sinusoidal behavior in region A for a higher S/N ratio or larger size of A. Therefore, the extended correlation functions by the ME method for such cases tend to be longer and thus require longer DFTs. To further illustrate this point with specific examples, we have considered a case in which $\sigma^2 = 0.5$ with all other parameters to be the same as in Table 3 and another case in which the size of A is 7×7 with all other parameters to be the same as in Table 3. To obtain the desired ME PS estimate, both cases required the DFT size of 128×128.

If there is significant aliasing error relative to the ε used for the convergence test, then the algorithm does not converge. For example, if the DFT size of 32×32 is used for the example of Figure 7, the algorithm does not converge. In such a case, the DFT length has to be increased to obtain the ME PS estimate. If the DFT length can not be increased due to computational constraints, ε has to be increased to tolerate a larger aliasing error. In such a case, the resulting PS estimate will only be an approximation to the ME PS estimate.

In general, cases in which the S/N ratio is lower or the size of A is smaller require less computations to reach the desired ME PS estimate for two reasons. One reason is that such cases require shorter DFT lengths, as are clear from Table 4. Another reason is that a larger noise power (σ^2) contributes a larger positive spectral component in the correlation correction step and the Fourier transform of a smaller rectangular window has a smaller amplitude in its negative lobe. The effect of this is generally a smaller value of α in each iteration and therefore more ideal correction of the correlation function in each iteration. Consequently, for such cases, a smaller number of iterations is required to reach the ME PS estimate. In fact, when the S/N ratio is sufficiently low and the size of A is sufficiently small, the value of α can be chosen to be 0 in all iterations and the computation time can be significantly reduced. As an example, we have considered a case in which $\sigma^2 = 6.0$ and size of A = 3×3 with all other parameters to be the same as in Table 3. The computation time required in generating the ME PS estimate for this case was 4.5 seconds of CPU time using IBM 370 at M.I.T. Lincoln Laboratory. This is significantly shorter than 75 seconds required to generate the result in Figure 7(c).

Two additional examples of 2-D ME PS estimates are shown in Figures 8 and 9. The results in these two figures were obtained using the parameters in Tables 5 and 6 respectively.

In addition to the above examples, we have considered a variety of others. In all cases that we have considered so far, we have empirically observed that the algorithm always converges to the ME PS estimate for a sufficiently large choice of DFT length and a sufficiently small choice of ε. In addition, we have also observed that the ME PS estimates for 2-D signals have high resolution characteristics similar to the 1-D case. A more quantitative study on the high resolution characteristics of the ME PSE method for 2-D signals is currently under investigation.

In this paper, we have developed a specific numerical algorithm to estimate the power spectrum of a signal by the ME method. Even though this algorithm led to successful results, there is considerable room for further imporvements of the algorithm. For example, to avoid the spectral zero crossing problem in both the correlation domain and the coefficient domain, we have considered a smaller correction only in the correlation domain. An alternative approach

TABLE 5

Parameters of a two-dimensional example for Figure 8.
Notations used in the table are explained in Table 1.

A	M	σ^2	a_i^2	$(\omega_{i1}/2\pi, \omega_{i2}/2\pi)$	ε	NDFT	NITR	Time
5 5	2	2.0	2.0 1.0	0.3333 0.20 0.10 0.22	10^{-4}	64×64	71	26.8 secs.

TABLE 6

Parameters of a two-dimensional example for Figure 9.
Notations used in the table are explained in Table 1.

A	M	σ^2	a_i^2	$(\omega_{i1}/2\pi, \omega_{i2}/2\pi)$	ε	NDFT	NITR	Time
7×7	3	6.0	1.0 1.0 1.0	0.10 0.10 0.30 0.10 0.20 0.20	10.4	32×32	42	5 secs.

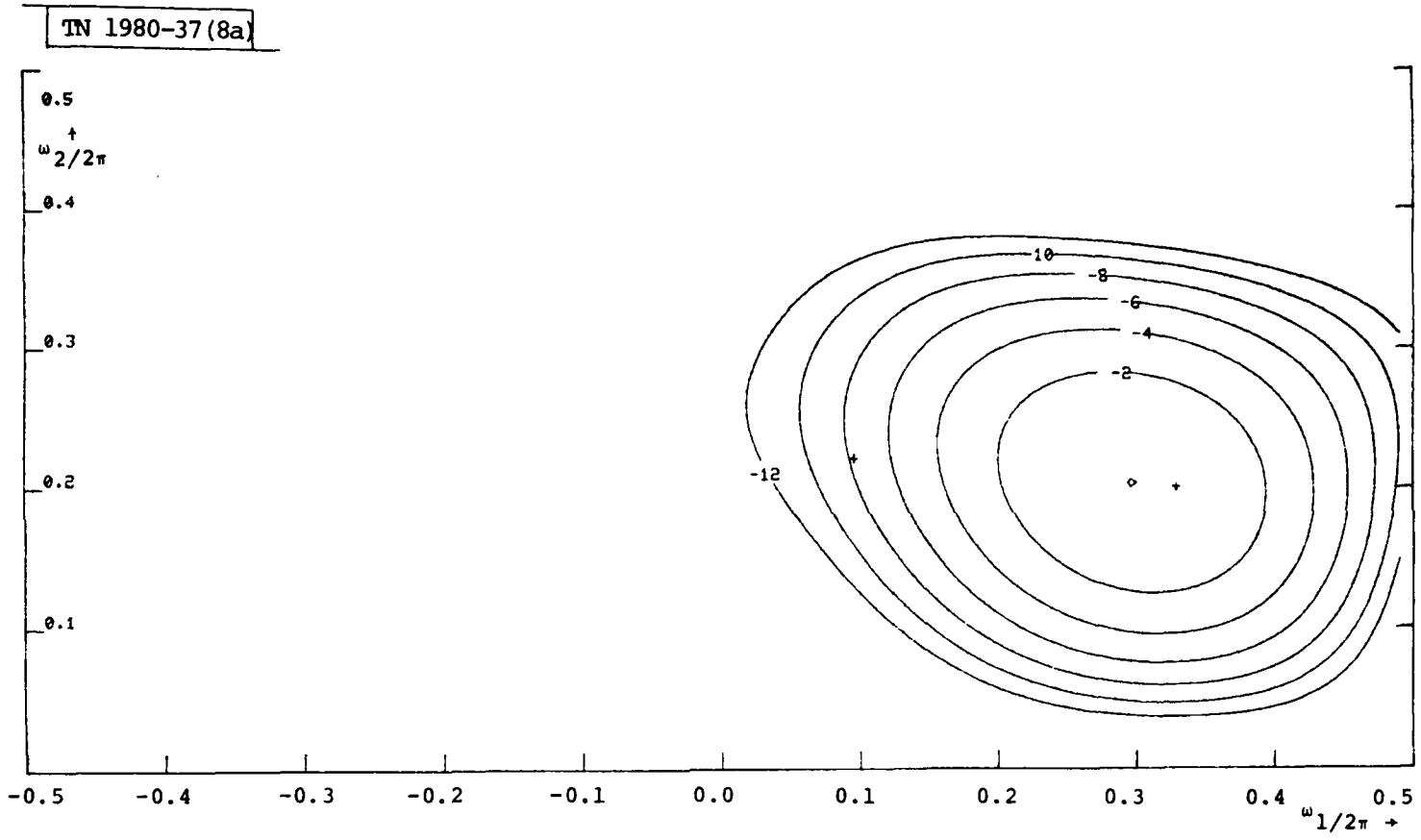

(a) Result of PSE by periodogram.

Fig. 8. 2-D PSE for data in Table 5.

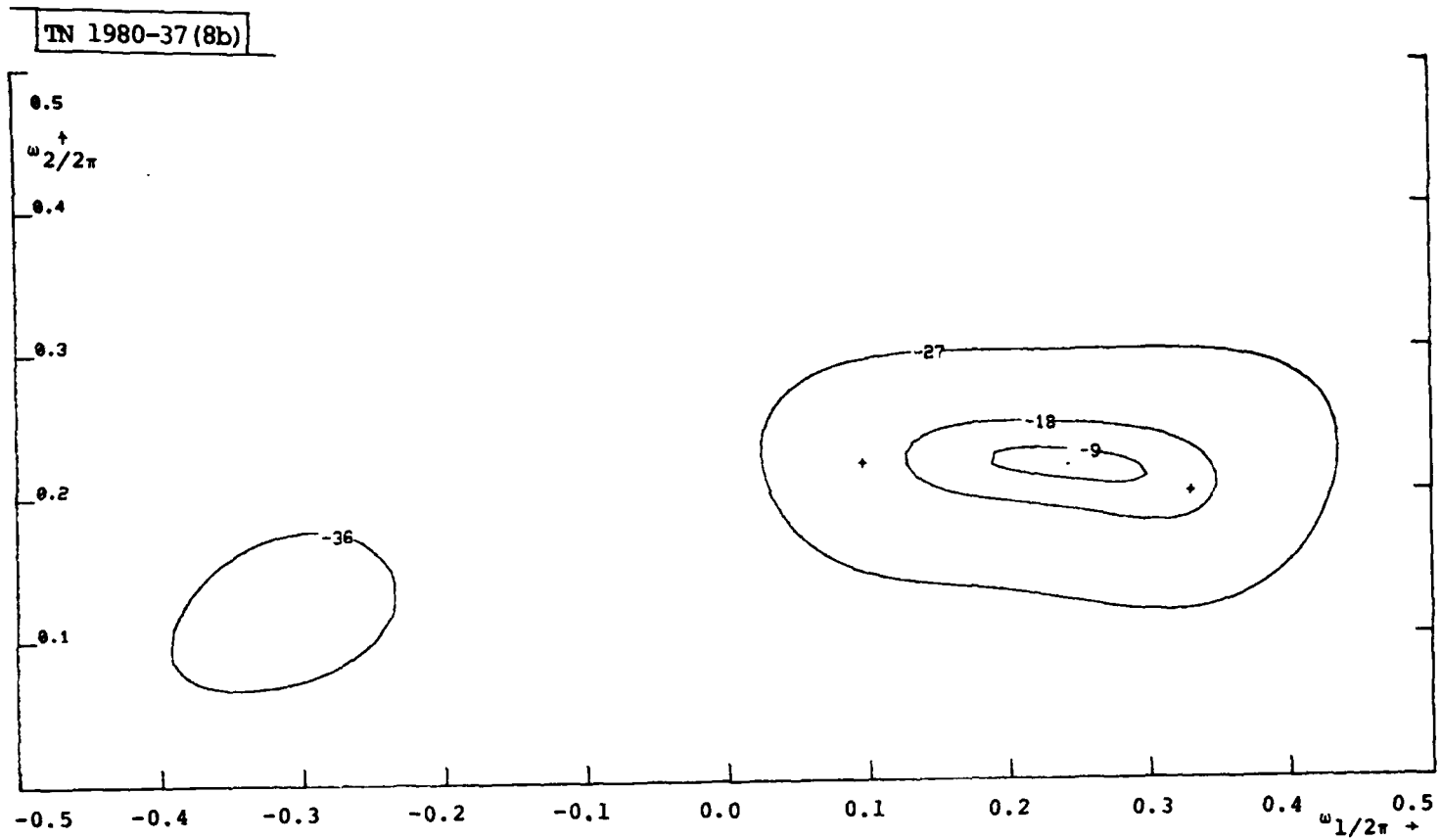

(b) Result of PSE based on the backward L auto-regressive filter.

Fig. 8. Continued.

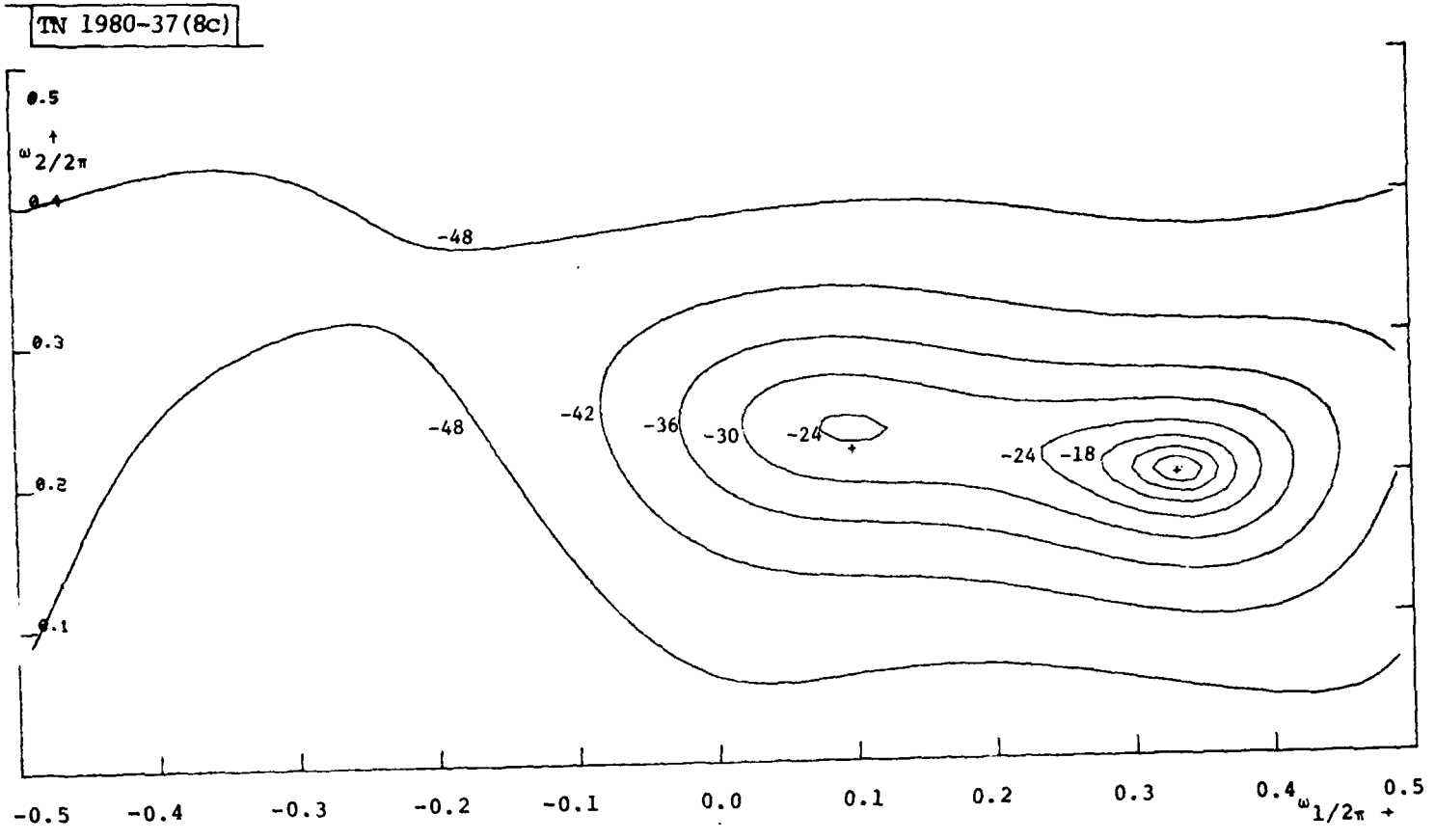

(c) ME PS estimate by the iterative algorithm in Fig. 4.

Fig. 8. Continued.

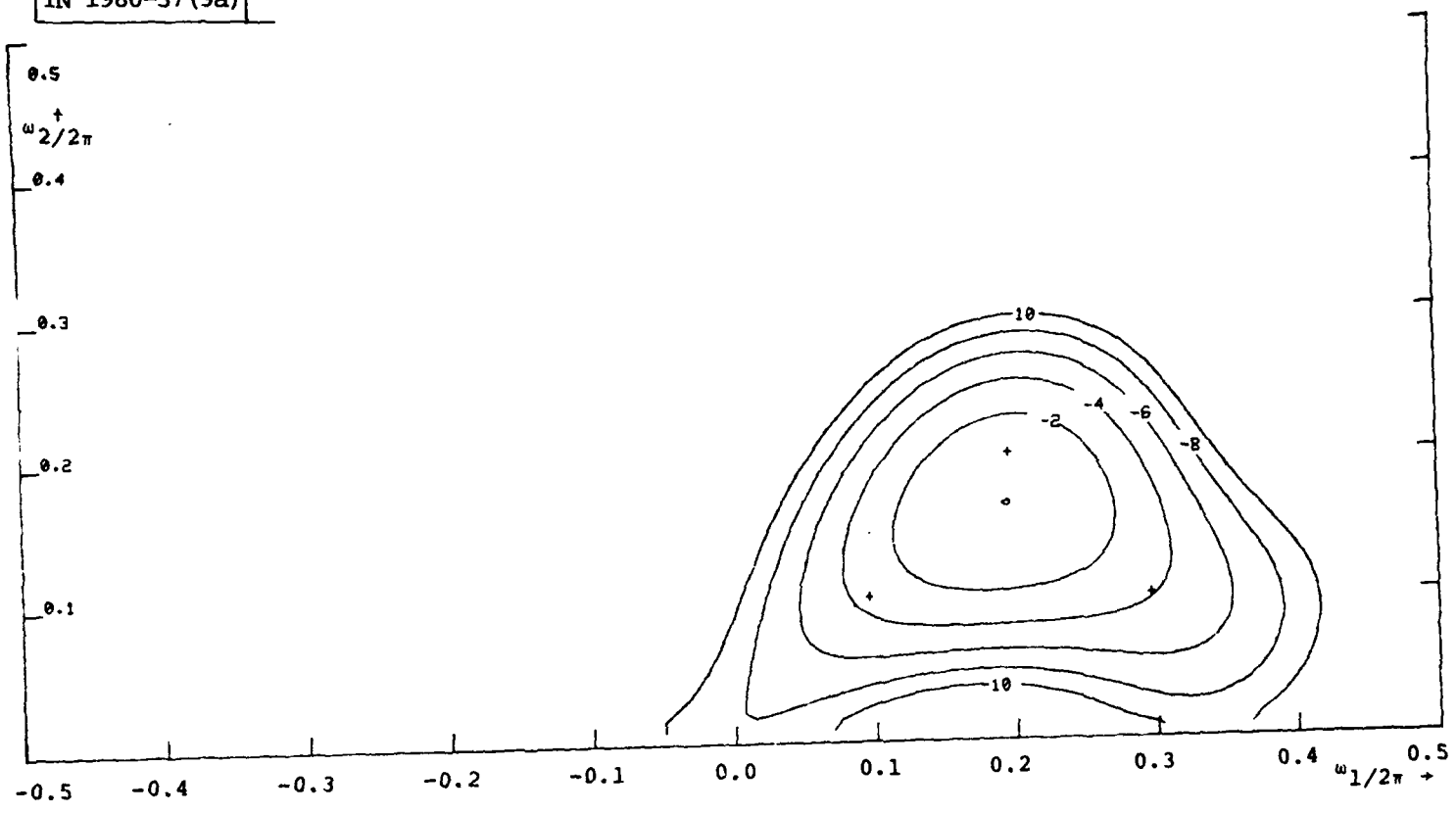

(a) Result of PSE by periodogram.

Fig. 9. 2-D PSE for data in Table 6.

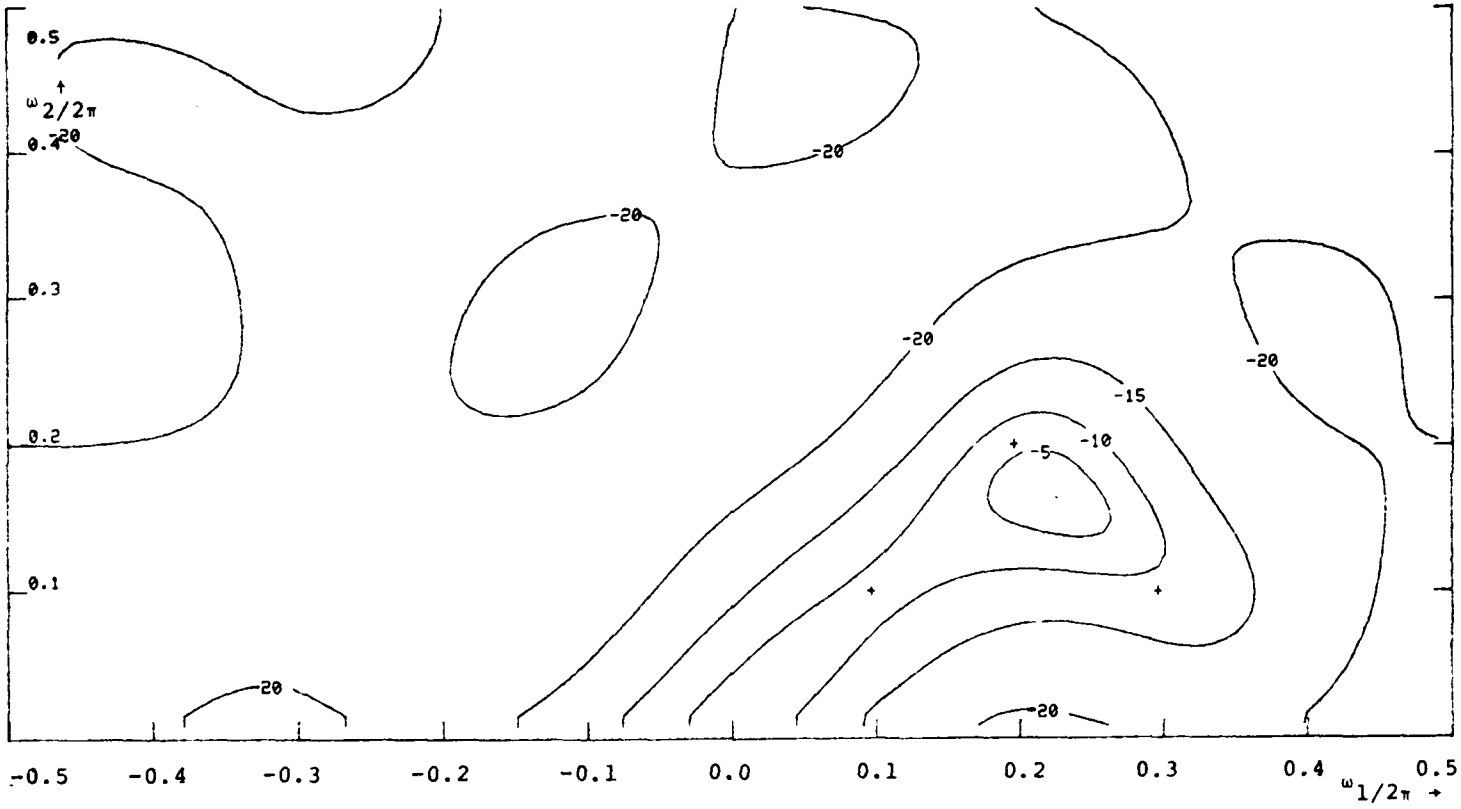

(b) Result of PSE based on the backward L auto-regressive filter.

Fig. 9. Continued.

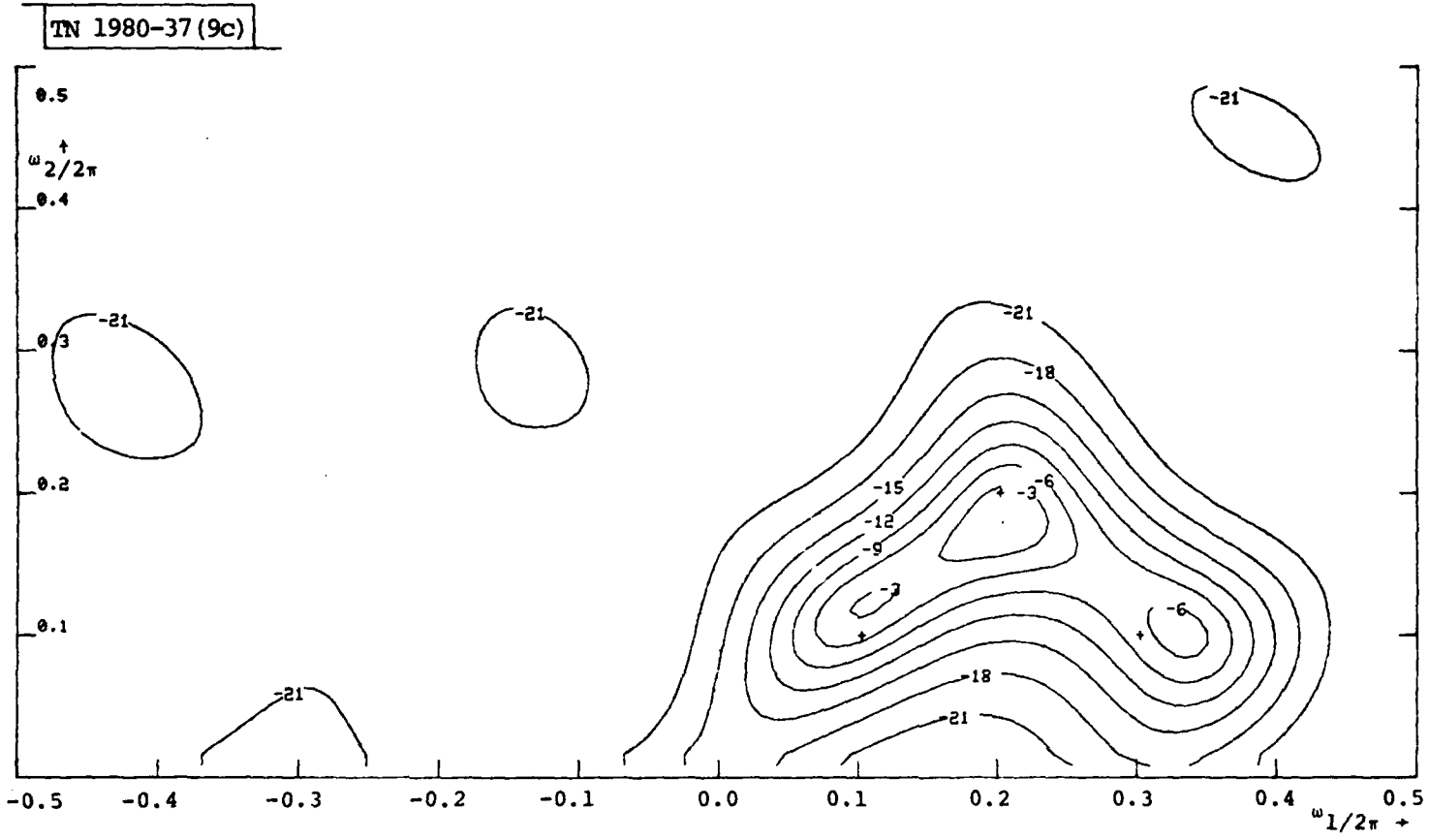

(c) ME PS estimate by the iterative algorithm in Fig. 4.

Fig. 9. Continued.

would be to perform a smaller correlation correction and a smaller coefficient correction to avoid the spectral zero crossing problems in the correlation and coefficient domains respectively. Such an approach may allow more optimum choice of the parameters such as α without significant computational burden. This and other ways to improve the performance of the algorithm are currently under investigation.

Finally, in this report, we have considered the ME PSE of only 1-D and 2-D signals. However, the iterative algorithm developed is based on the notion that the ME PS estimate should be consistent with the given correlation points in the region A and the corresponding coefficients should be zero outside the region A, which can be applied to signals of all dimensions. Consequently, the iterative algorithm developed in this paper may also be useful for the ME PSE of signals whose dimensions are higher than two.

ACKNOWLEDGEMENT

The authors acknowledge valuable discussions with Professor James H. McClellan, Professor Alan V. Oppenheim, and Dr. Dan E. Dudgeon.

REFERENCES

[1] J., Makhoul, "Spectral Analysis of Speech by Linear Prediction," IEEE Trans. Audio Electroacoust., AU-21, 140-148 (1973).

[2] J.W. Woods, "Two Dimensional Markov Spectral Estimation," IEEE Trans. on Info. Th., IT-22, 552-559 (1976).

[3] H.C. Andrews, and B.R. Hunt, Digital Image Restoration (Prentice-Hall, New Jersey, 1977), pp. 90-112.

[4] J.H. McClellan, and R.J. Purdy, "Applications of Digital Signal Processing to Radar," in Applications of Digital Signal Processing, edited by A.V. Oppenheim, (Prentice-Hall, New Jersey, 1978), pp. 239-326.

[5] A.B. Baggeroer, "Sonar Signal Processing," in Applications of Digital Signal Processing, edited by A.V. Oppenheim, (Prentice Hall, New Jersey, 1978) pp. 331-428.

[6] S.F. Gull, and G.J. Daniell, "Image Reconstruction From Incomplete and Noisy Data," Nature, 272, 686-690 (1978).

[7] J. Makhoul, "Linear Prediction: A Tutorial Review," Proc. IEEE, 63, 561-580, April,1975.

[8] A.V. Oppenheim, R.W. Schafer, Digital Signal Processing, (Prentice-Hall, New Jersey, 1975), pp.532-571.

[9] P.D. Welch, "The Use of Fast Fourier Transform For The Estimation of Power Spectra: A Method Based On Time Averaging Over Short, Modified Periodograms," IEEE Trans. on Audio Electroacoust. AU-15, 70-73, (1976).

[10] R.T. Lacoss, "Data Adaptive Spectral Analysis Methods," Geophysics, 36, 661-675 (1971).

[11] J.P. Burg, unpublished notes, 1974. See pp. 20-21 of Ref. 17 below.

[12] S.J. Wernecke and L.R. D'Addario, "Maximum Entropy Image Reconstruction," IEEE Trans. Comp. C-26, 351 (1974).

[13] W.I. Newman, "A New Method of Multidimensional Power Spectral Analysis," Astronomy and Astrophysics 54, 369 (1977).

[14] B.W. Dickinson, "Two-Dimensional Markov Spectrum Estimates Need Not Exist," to appear in IEEE Trans. Information Theory

[15] R.W. Gerchberg, and W.D. Saxton, "A Practical Algorithm for the Determination of Phase from Image and Diffraction Plane Pictures," Optik, 35 237-246 (1972).

[16] J.R. Fienup, "Reconstruction of an Image from the Modulus of its Fourier Transform," Optics Letters, 3 27-29 (1978).

[17] J.V. Pendrell, "The Maximum Entropy Principle in Two Dimensional Spectral Analysis," PhD. Thesis, York University, Ontario, Canada, (November 1979), pp. 210-219.

(14) TN-1980-37

(16) 7820

UNCLASSIFIED

SECURITY CLASSIFICATION OF THIS PAGE (When Data Entered)

(19) REPORT DOCUMENTATION PAGE

READ INSTRUCTIONS BEFORE COMPLETING FORM

(1) (2) 1. REPORT NUMBER: ESD-TR-80-92	2. GOVT ACCESSION NO. AD-A092128 — 3. RECIPIENT'S CATALOG NUMBER
(6) 4. TITLE (and Subtitle): A New Algorithm for Two-Dimensional Maximum Entropy Power Spectrum Estimation	(9) 5. TYPE OF REPORT & PERIOD COVERED: Technical Note 6. PERFORMING ORG. REPORT NUMBER: Technical Note 1980-37
(10) 7. AUTHOR(S): Jae S. Lim, Naveed A. Malik	(15) 8. CONTRACT OR GRANT NUMBER(S): F19628-80-C-0002, N00014-75-C-0951/NR049-328
9. PERFORMING ORGANIZATION NAME AND ADDRESS: Lincoln Laboratory, M.I.T., P.O. Box 73, Lexington, MA 02173 — M.I.T., Research Laboratory of Electronics, Cambridge, MA 02139	10. PROGRAM ELEMENT, PROJECT, TASK AREA & WORK UNIT NUMBERS: Program Element No. 33401F, Project No. 7820
11. CONTROLLING OFFICE NAME AND ADDRESS: Defense Advanced Research Projects Agency, 1400 Wilson Boulevard, Arlington, VA 22209 — Air Force Systems Command, USAF, Andrews AFB, Washington, DC 20331	(11) 12. REPORT DATE: 7 August 1980 13. NUMBER OF PAGES: 56
14. MONITORING AGENCY NAME & ADDRESS (if different from Controlling Office): Electronic Systems Division, Hanscom AFB, Bedford, MA 01731 — Office of Naval Research, 800 N. Quincy Street, Arlington, VA 22217	15. SECURITY CLASS. (of this report): Unclassified (12) (55) 15a. DECLASSIFICATION DOWNGRADING SCHEDULE

16. DISTRIBUTION STATEMENT (of this Report)

Approved for public release; distribution unlimited.

17. DISTRIBUTION STATEMENT (of the abstract entered in Block 20, if different from Report)

18. SUPPLEMENTARY NOTES

None

19. KEY WORDS (Continue on reverse side if necessary and identify by block number)

power spectrum estimation
two-dimensional power spectrum estimation
maximum entropy method
two-dimensional maximum entropy method
signal processing

20. ABSTRACT (Continue on reverse side if necessary and identify by block number)

A new iterative algorithm for the maximum entropy power spectrum estimation is presented in this report. The algorithm, which is applicable to two-dimensional signals as well as one-dimensional signals, utilizes the computational efficiency of the Fast Fourier Transform (FFT) algorithm and has been empirically observed to solve the maximum entropy power spectrum estimation problem. Examples are shown to illustrate the performance of the new algorithm.

DD FORM 1 JAN 73 1473 EDITION OF 1 NOV 65 IS OBSOLETE

UNCLASSIFIED

SECURITY CLASSIFICATION OF THIS PAGE (When Data Entered)

207650 JM


LMED
8